Beyond Dirac Fermions

Dublin Institute for Advanced Studies

Abdulhakim Mohd Nazir

In collaboration with Tomás Lannon

Supervisor: Dr. Giandomenico Palumbo

August 6, 2023

Abstract

In this project, we study the nature of both the Dirac fermions and the unconventional Dirac-like fermions. Dirac fermions are a principal contributor to both particle physics and condensed matter systems, especially topological quantum matter/materials. The Dirac matrices, α_μ, and the Clifford algebra $\mathrm{Cl}_{3,1}$ that they generate, govern the heart of the Dirac theory. The Clifford algebra $\mathrm{Cl}_{3,1}$ is characterised by the following anti-commutation relations $\{\alpha_\mu, \alpha_\nu\} = 2\delta_{\mu\nu}\mathbb{1}$, where $\delta_{\mu\nu}$ is the Kronecker delta and $\mathbb{1}$ is the identity matrix. An investigation is conducted in order to construct different matrices, β_μ, which do not generate the Clifford algebra $\mathrm{Cl}_{3,1}$. The purpose of β_μ is to replace α_μ for our proposed Dirac-like model. These different matrices can be used to describe exotic Dirac-like fermions, facilitating the construction of new theoretical fermionic models. The natural environment of these exotic fermion types would be condensed matter systems, which impose different symmetry constraints to relativistic particles, allowing for fermion types beyond the standard categories of Dirac, Majorana and Weyl in quantum field theory (QFT).

In this project, both the Dirac theory and Dirac-like model of fermions is taken in 3+1 dimensions, $X = \mathbb{R}^4$ spacetime. In 3+1 dimensions, α_μ are the 4×4 Dirac matrices for the Dirac theory. For our proposed Dirac-like model, β_μ are $n \times n$ matrices, where $5 \leq n \leq 8$. The 3+1-dim Dirac theory includes a single mass term, m_1, while our Dirac-like model has two independent mass terms, m_1 and m_2. The matrices, α_μ and β_μ, are used to construct a resultant density Hamiltonian $\mathcal{H}$ which yield eigenvalues corresponding to the energies of the fermionic systems, upon diagonalisation of $\mathcal{H}$. We also explicitly calculate the spin matrices of S_i generators for the spin-s representation of $SO(3)$ symmetry, in which our model follows. We further investigate the real spectra of the resulting energy dispersion relations $E(k)$ as well as the possibility of bullding a β_6 matrix associated with a third independent mass term m_3.

Acknowledgements

First and foremost, I would like to express my sincere gratitude to my project supervisor Dr. Giandomenico Palumbo for proposing this investigation as a summer research project. His immense knowledge, motivation and enthusiasm sparked a tremendous interest in considering condensed matter physics as a potential career option to specialise in. His guidance throughout this project was absolutely crucial in order to both understand the subject matter and develop the methods used to achieve the desired goals. His brilliance as a supervisor cannot be understated, and I would like to continue working with him in the near future.

Furthermore, I would like to sincerely thank the project coordinators Dr. Atri Dey and Dr. Saki Koizumi for their outstanding support, patience and management of the entirety of the summer research projects. Especially Saki with her insightful advice and tireless commitment to reviewing my written reports. Her comments have proved extraordinarily helpful and her dedication to assist with the project is absolutely praiseworthy. I also need to thank the director of the DIAS School of Theoretical Physics, Prof. Denjoe O'Connor for offering me the position of this summer research internship. It would be a great pleasure to continue being involved with DIAS, since I feel an experienced academic such as Denjoe can offer so much guidance, wisdom and knowledge, and by extension, the entirety of the DIAS staff can aswell.

Additionally, I would like to show my unwavering joy and appreciation of collaborating with my research partner Tomás Lannon. His readiness to work as a team and deliver exceptional contributions towards our project goals cannot be highlighted enough. His mathematical skills and knowledge proved instrumental, and his character and conduct ensured a pleasant experience. I'm proud to call him my friend.

Last but not least, I would like to acknowledge my family. I can only hope to become someone that they can be proud of in the future.

Contents

List of Figures

Chapter 1

The Model

1.1 Motivation Behind the Project

As mentioned in the abstract, the Dirac fermions play a fundamental role in both particle physics and condensed matter physics, especially with regards to topological quantum matter. The project involves the further investigation of unconventional Dirac-like fermions which have the potential to construct new theoretical models, a rich and active area that is especially prevalent in condensed matter physics. Condensed matter systems serve as a natural arena for the discovery of fermionic particles, in the form of quasiparticle excitations. An example of potential uses includes the topological protection of quantum information, which can play a role in topological quantum computing.

Topological systems are systems with some quantum information stored non-locally and the fermionic excitations or emergent quasiparticles are topologically protected. They are robust to decoherence from local quantum interference, which prompts potential use for topological quantum computation. An example of this is outlined in [6] which includes the use of a toy model called the Kitaev chain (KC). A toy model is a theoretical model constructed in order to highlight the most important features of a physical system although it is not supposed to directly correspond to it. The KC is 1-D fermionic chain and the sites can be occupied or unoccupied by an electron, which is insulating in the bulk (infinite system/periodic boundary conditions) and also has a superconducting gap. In the topological phase, the chain possesses exponentially localised zero energy bound states. This is quite interesting in the Majorana representation of the Kitaev chain. The subsitution of the Majorana basis into the Kitaev Hamiltonian results in a non-local fermionic state that is essentially decoupled from the rest of the states. Majorana states are described to be exponentially well-localised and low energy at the end of the chain. The reconstruction of an entire fermion is only possible when you take the two Majorana states at the end of the fermionic chain. However, one is unable to decohere the quantum information of the

cubit using local perturbations. They would need to perform something simultaneously to both ends of the chain in a quantum coherent way in order to perturb this zero energy state. Thus the topological system is robust. Experimental evidence was reported from a quantum wire sitting on a superconductor which featured Majorana zero modes observed at the end of the chain as theorised [1]. The toy model really illustrates the fractionalization of electrons into these effective quasiparticles, which are Majorana fermions.

Majorana fermions also featured in the Sachdev-Ye-Kitaev (SYK) model [7], which is a model that was also implemented to approach the problem of quantum gravity. It bears close relevance to the AdS/CFT discrete model which is utilised in theories of quantum gravity constructed in terms of string/M-theory and conformal field theories (CFT) for describing elementary particles. It consisted of N interacting Majorana fermions χ_j satisfying the Clifford relation $\{\chi_k, \chi_j\} = 2\delta_{ij}$, with the most famous model defined as $H_{SYK} = \frac{1}{4!}\sum_{j,k,l,m} J_{jklm}\chi_j\chi_k\chi_l\chi_m$.

The following is based from a research paper [2] which essentially incentivised this investigation. In quantum field theory (QFT), fermions are classified as three types: Dirac, Majorana (fermions which are their own antiparticle) and Weyl (massless fermions). Condensed matters systems are a potential ground for observing fermionic particles and phenomena, which can have a high energy counterpart. Relativistic fermions are constrained by Poincaré symmetry, which is the full symmetry of special relativity. However in condensed matter systems, the fermions are not constrained by Poincaré symmetry. Instead, they must only conform to the crystal symmetry of one of the 230 space groups (SG) of the 3-D lattices, providing less constraint on the types of particles that can arise. Thus, there is potential to observe and categorise free fermionic excitations in solid state physics which have no counterpart in high energy physics. Possible exotic fermion types can exist beyond the three classifications of fermions: Dirac, Majorana and Weyl. These fermions can describe fascinating surface states, such as Fermi arcs and Dirac lines, ARPES (angle-resolved photoemission spectroscopy) signatures and magnetotransport properties of many material candidates with time-reversal (TR) symmetry and spin-orbit coupling.

This project involves calculating the eigensystem of the Dirac-like model to obtain the energies of these free fermionic systems. The real spectrum of the resulting energy dispersion relations $E(k)$ would then be subsequently plotted using the computational software Wolfram Mathematica. The investigation is also conducted in order to determine a possible β_6 matrix related to a third mass term, m_3, in our proposed Dirac-like model in 3+1 dimensions.

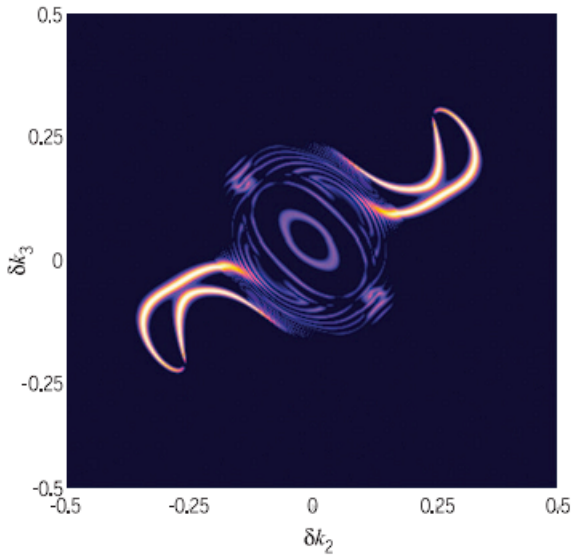

Figure 1.1: Surface Fermi arcs of a threefold degeneracy in SG 214 as seen from [2]. The figure outlines the surface density of states as a function of momentum for a conventional crystal.

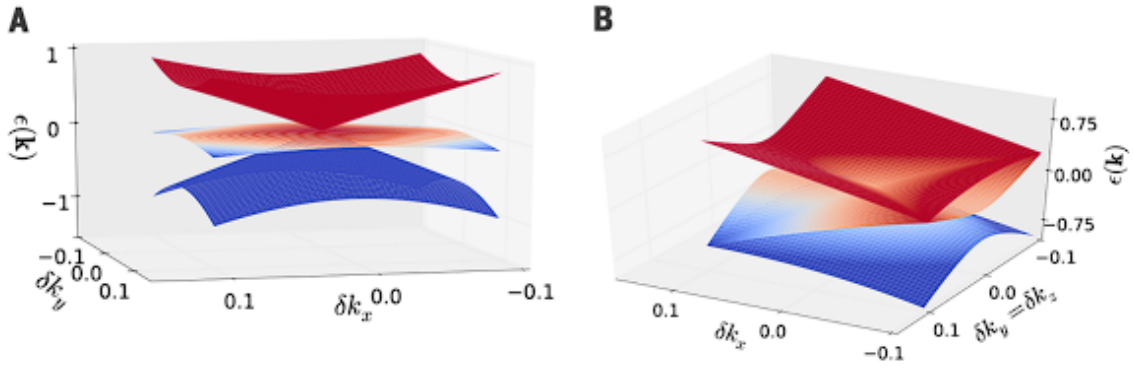

Figure 1.2: Energy dispersion relations $E(k)$ near a threefold degeneracy at a high symmetry point, as illustrated from [2]. (A) represents SGs 199 and 214 and (B) represents SG 220.

1.2 Introduction to Relativistic Wave Equations

In this section, some background context [3] is introduced for relativistic wave equations, that would be somewhat relevant to our investigation. Since the 1920's, physicists have yearned to develop a relativistic description of a quantum mechanical system. The earliest known case of utilising Lorentz invariance, a relativistic concept, with quantum mechanics, was pioneered by Louis de Broglie in 1923, for the purpose of constructing the familiar relations between the energy/momentum of a particle and the frequency/wave vector of the corresponding wave. As a matter of fact, Erwin Schrödinger initially developed a relativistic version of his famous Schrödinger equation, now referred to as the Klein-Gordan equation, named after Oskar Klein and Walter Gordon. Schrödinger analysed the relativistic energy-momentum relation for an electron

$$-\frac{W^2}{c^2} + p^2 + m^2c^2 = 0 \tag{1.1}$$

and then considered a wavefunction $\psi(x,t)$, which describes the electron, as a solution by making quantum mechanical substitutions

$$\frac{W}{c} \Longrightarrow \frac{i\hbar}{c}\frac{\partial}{\partial t}, \qquad \mathbf{p} \Longrightarrow -i\hbar\nabla \tag{1.2}$$

yielding the first relativistic wave equation, the Klein-Gordan (KG) equation

$$\left(\Box + \frac{m^2c^2}{\hbar^2}\right)\psi = 0 \tag{1.3}$$

where $\Box$ is the d'Alembert operator

$$\Box = \partial^\mu\partial_\mu = \eta^{\mu\nu}\partial_\nu\partial_\mu = \frac{1}{c^2}\frac{\partial^2}{\partial t^2} - \frac{\partial^2}{\partial x^2} - \frac{\partial^2}{\partial y^2} - \frac{\partial^2}{\partial z^2} \tag{1.4}$$

$$= \frac{1}{c^2}\frac{\partial^2}{\partial t^2} - \nabla^2 = \frac{1}{c^2}\frac{\partial^2}{\partial t^2} - \Delta \tag{1.5}$$

and $\nabla^2 := \Delta$ is the 3-D Laplacian and $\eta^{\mu\nu}$ is the inverse Minkowski metric.

However, the failure of the KG equation to experimentally verify the fine structure of the energy levels of the hydrogen atom, led Schrödinger to initially discard this result. However, in the non-relativistic limit, it produced the standard Schrödinger equation which proved famous and successful. The discrepancy between theory and experiment was due to the spin of the electron, in which Schrödinger neglected. However, the issue of possible negative probabilites associated with the KG equation with its second-order derivative with respect to time, inspired Paul Dirac to develop a relativistic wave equation which was first-order differential. He proposed assumptions such as

the space derivatives being well linear in the wave equation in order to develop a consistent Lorentz-invariant theory, leading to the following expression

$$\left(\frac{W}{c} + \alpha \cdot p + \alpha_0 mc\right)\psi = 0 \tag{1.6}$$

His introduced α notation, which act as dynamical variables, were required to fulfil the desired condition of the problem, that the energy and momentum of the particle verified the relativistic energy-momentum relation in Eq. (1.1). This is also equivalent to the fact that the solution of the Dirac equation likewise satisfies the KG equation. Another problem that Dirac wanted to rectify was the issue of the negative energy states of the KG equation, but we will not go into detail in this report. The Dirac theory proved overwhelmingly successful as it provided correct predictions for the fine structure of the hydrogen atom and the correct value of the magnetic moment of the electron, with predicted gyromagnetic ratio $g = 2$. The nature of α, which serve as the novel dynamical variables, will be addressed in the following sections. As what was reviewed here, one can develop some understanding of the role of α in the Dirac theory in 3+1 dimensions and then translate that to β in our proposed Dirac-like theory in 3+1 dimensions.

1.3 Dirac Theory in 3+1 Dimensions

The Dirac theory of fermions in 3+1 dimensions can be described by the following Hamiltonian

$$H = \psi^\dagger \mathcal{H} \psi \tag{1.7}$$

where $\psi = (\psi_1, \psi, \ldots, \psi_n)^T$ is a n-component spinor with $n = 2^s$, while the density Hamiltonian $\mathcal{H}$ can be written as the following

$$\mathcal{H} = \alpha_i p_i + \alpha_0 m \tag{1.8}$$

where m is the Dirac mass, $p_i = (p_x, p_y, p_z)$ are the momenta and $\alpha_\mu = (\alpha_0, \alpha_x, \alpha_y, \alpha_z)$ are Dirac matrices that satisfy the following Clifford algebra $\mathrm{Cl}_{3,1}$

$$\{\alpha_\mu, \alpha_\nu\} \equiv \alpha_\mu \alpha_\nu + \alpha_\nu \alpha_\mu = 2\delta_{\mu\nu}\mathbb{1} \tag{1.9}$$

where $\delta_{\mu\nu}$ is the Kronecker delta and $\mathbb{1}$ is the identity matrix. One can prove that α_μ are even-order $2^s \times 2^s$, as outlined in Sect.(1.3.1), where s is some positive integer. Upon diagonalisation of the density Hamiltonian $\mathcal{H}$, the following eigenvalues are obtained

$$E_-^j = -\sqrt{p_x^2 + p_y^2 + p_z^2 + m^2}, \qquad E_+^j = \sqrt{p_x^2 + p_y^2 + p_z^2 + m^2} \tag{1.10}$$

where j is the degeneracy of the eigenvalues. One can recognise these eigenvalues as the expression for the relativistic energy-momentum relations as seen in Eq. (1.1),

where $\hbar = c = 1$ in natural units.

As explained in (1.3.1), in 3+1 dimensions, $s = 2$ which means that $j = 2$. This is evident from the Dirac matrices as seen in (1.3.1), which are 4×4 matrices, that compose the density Hamiltonian $\mathcal{H}$

$$\mathcal{H} = \begin{bmatrix} m & 0 & p_z & p_x - ip_y \\ 0 & m & p_x + ip_y & -p_z \\ p_z & p_x - ip_y & -m & 0 \\ p_x + ip_y & -p_z & 0 & -m \end{bmatrix} \tag{1.11}$$

which yield the following eigenvalues upon diagonalisation

$$E = \pm\sqrt{p_x^2 + p_y^2 + p_z^2 + m^2}, \qquad E = \pm\sqrt{p_x^2 + p_y^2 + p_z^2 + m^2} \tag{1.12}$$

1.3.1 Properties of the Matrices α_i and α_0

The intended purpose of this subsection is to just provide context to the α_μ matrices involved in the Dirac theory of 3+1 dimensions, which would hopefully be relevant to the β_μ matrices in our investigation of the Dirac-like model in 3+1 dimensions. From the description of the free Dirac particle, there follows a number of resulting properties as proposed by Dirac

1. H is Hermitian: $\hat{H} = H^\dagger$. Requirement that α_i and α_0 are also Hermitian: $\alpha_i = \alpha_i^\dagger$ and $\alpha_0 = \alpha_0^\dagger$.
2. α_i and α_0 are square matrices: $\alpha_i, \alpha_0 \in M_n(\mathbb{C})$.
3. α_i and α_0 yield eigenvalues ± 1 ($\alpha_i^2 = \alpha_0^2 = \mathbb{1}$).
4. α_i and α_0 are constant matrices. They do not depend on $\vec{r}$ and t.
5. Anti-commutation relations: $\{\alpha_i, \alpha_j\} = \{\alpha_i, \alpha_0\} = 0$.
6. The trace of the matrices α_i and α_0 are zero: $\mathrm{Tr}(\alpha_i) = 0$ and $\mathrm{Tr}(\alpha_0) = 0$.
7. α_i and α_0 are even-order matrices: $2^s \times 2^s$, where s is some positive integer. This follows from conditions 2, 3 and 6.

It is evident that in 3+1 dimensions, the lowest value of s is 2. Consider the following observation. The well known Pauli spin matrices satisfy all the seven conditions and so one is tempted to construct a 2×2 representation in terms of the Pauli matrices

$$\sigma_x = \begin{bmatrix} 0 & 1 \\ 1 & 0 \end{bmatrix} \qquad \sigma_y = \begin{bmatrix} 0 & -i \\ i & 0 \end{bmatrix} \qquad \sigma_z = \begin{bmatrix} 1 & 0 \\ 0 & -1 \end{bmatrix} \tag{1.13}$$

However using this representation, it is impossible to construct α_0 that satisfies all seven conditions. In the Dirac theory in 3+1 dimensions, four matrix components are required $\alpha_x, \alpha_y, \alpha_z, \alpha_0$. And so with the inability to construct α_0 in the 2×2 representation, the next available representation is 4×4. Thus the lowest value of s is 2 in 3+1 dimensions.

There are numerous examples of 4×4 matrices that satisfy the Clifford algebra $\mathrm{Cl}_{3,1}$ $\{\alpha_\mu, \alpha_\nu\} = 2\delta_{\mu\nu}\mathbb{1}$. One such 4×4 representation is also known as the *Pauli-Dirac* representation with α_i and α_0 expressed as the following

$$\alpha_x = \begin{bmatrix} 0 & 0 & 0 & 1 \\ 0 & 0 & 1 & 0 \\ 0 & 1 & 0 & 0 \\ 1 & 0 & 0 & 0 \end{bmatrix} = \begin{bmatrix} \underline{0} & \sigma_x \\ \sigma_x & \underline{0} \end{bmatrix} \quad \alpha_y = \begin{bmatrix} 0 & 0 & 0 & -i \\ 0 & 0 & i & 0 \\ 0 & -i & 0 & 0 \\ i & 0 & 0 & 0 \end{bmatrix} = \begin{bmatrix} \underline{0} & \sigma_y \\ \sigma_y & \underline{0} \end{bmatrix} \tag{1.14}$$

$$\alpha_z = \begin{bmatrix} 0 & 0 & 1 & 0 \\ 0 & 0 & 0 & -1 \\ 1 & 0 & 0 & 0 \\ 0 & -1 & 0 & 0 \end{bmatrix} = \begin{bmatrix} \underline{0} & \sigma_z \\ \sigma_z & \underline{0} \end{bmatrix} \quad \alpha_0 = \begin{bmatrix} 1 & 0 & 0 & 0 \\ 0 & 1 & 0 & 0 \\ 0 & 0 & -1 & 0 \\ 0 & 0 & 0 & -1 \end{bmatrix} = \begin{bmatrix} \mathbb{1} & \underline{0} \\ \underline{0} & -\mathbb{1} \end{bmatrix} \tag{1.15}$$

where $\underline{0}$ is the 2×2 zero-matrix and $\mathbb{1}$ is the 2×2 identity matrix.

Using these matrices, it is clear that they construct the density Hamiltonian $\mathcal{H}$ outlined in matrix (1.11) using Eq. (1.8).

Recall that the Dirac spinor $\psi = (\psi_1, \psi, \ldots \psi_n)^T$ is a n-component spinor with $n = 2^s$. With $s = 2$ in 3+1 dimensions, ψ can be represented as a 4-component "state"-function vector

$$|\psi(\vec{r}, t)\rangle = \begin{pmatrix} \psi_1(\vec{r}, t) \\ \psi_2(\vec{r}, t) \\ \psi_3(\vec{r}, t) \\ \psi_4(\vec{r}, t) \end{pmatrix} \tag{1.16}$$

where $|\psi(\vec{r}, t)\rangle$ does not transform like a "four-vector".

1.3.2 Lorentz Invariance of the Dirac Lagrangian

The following subsection is taken from [5], which provides the chain of reasoning or logical progression to delineate the full Lorentz invariance of the Dirac theory.

The transformation of a scalar field under a Lorentz transformation $x^\mu = (x')^\mu = \Lambda^\mu{}_\nu$ is as follows:

$$\phi(x) = \phi'(x) = \phi(\Lambda^{-1}x) \tag{1.17}$$

In general, a field can transform as

$$\phi^a(x) = D[\Lambda]^a{}_b\, \phi^b(\Lambda^{-1}x) \tag{1.18}$$

where the matrices $D[\Lambda]$ form a *representation* of the Lorentz group, meaning that

$$D[\Lambda_1]D[\Lambda_2] = D[\Lambda_1\Lambda_2] \tag{1.19}$$

and $D[\Lambda^{-1}] = D[\lambda]^{-1}$ and $D[1] = 1$. In order to find the different representations, we study the infinitesimal transformations of the Lorentz group and its resulting Lie algebra. By proposing

$$\Lambda^\mu{}_\nu = \delta^\mu{}_\nu + \omega^\mu{}_\nu \tag{1.20}$$

for infinitesimal ω, then the condition for a Lorentz transformation $\Lambda^\mu{}_\sigma\Lambda^\nu{}_\rho\eta^{\sigma\rho} = \eta^{\mu\nu}$ requires that ω is anti-symmetric

$$\omega^{\mu\nu} + \omega^{\nu\mu} = 0 \tag{1.21}$$

An anti-symmetric 4×4 matrix has $4 \times 3/2 = 6$ independent components that conforms with the 6 transformations of the Lorentz group: 3 rotations and 3 boosts. These 4×4 anti-symmetric matrices prove useful to be introduced as a basis, as represented by $(\mathcal{M}^{\rho\sigma})^\mu{}_\nu$ where anti-symmetric indices ρ, $\sigma = 0, ..., 3$. The anti-symmetry means that, for instance, $\mathcal{M}^{01} = -\mathcal{M}^{10}$. etc, so that ρ, σ label six different matrices. The basis of six 4×4 anti-symmetric matrices can be represented as

$$(\mathcal{M}^{\rho\sigma})^{\mu\nu} = \eta^{\rho\mu}\eta^{\sigma\nu} - \eta^{\sigma\mu}\eta^{\rho\nu} \tag{1.22}$$

Using these matrices for practical purposes typically requires lowering one index, via the Minkowski metric

$$(\mathcal{M}^{\rho\sigma})^{\mu\nu} = \eta^{\rho\mu}\delta^\sigma{}_\nu - \eta^{\sigma\mu}\delta^\rho{}_\nu \tag{1.23}$$

Two examples of these basis matrices are

$$(\mathcal{M}^{01})^\mu{}_\nu = \begin{bmatrix} 0 & 1 & 0 & 0 \\ 1 & 0 & 0 & 0 \\ 0 & 0 & 0 & 0 \\ 0 & 0 & 0 & 0 \end{bmatrix} \quad \textit{and} \quad (\mathcal{M}^{12})^\mu{}_\nu = \begin{bmatrix} 0 & 0 & 0 & 0 \\ 0 & 0 & -1 & 0 \\ 0 & 1 & 0 & 0 \\ 0 & 0 & 0 & 0 \end{bmatrix} \tag{1.24}$$

The first, $\mathcal{M}^{01}$ generates boosts in the x^1 direction. It is real and symmetric. The second $\mathcal{M}^{12}$ generates rotations in the (x^1, x^2)-plane. It is real and anti-symmetric. Thus, we can write any $\omega^\mu{}_\nu$ as a linear combination of $\mathcal{M}^{\rho\sigma}$

$$\omega^\mu{}_\nu = \frac{1}{2}\Omega_{\rho\sigma}(\mathcal{M}^{\rho\sigma})^\mu{}_\nu \tag{1.25}$$

where $\Omega^{\rho\sigma}$ are six numbers that tells us the nature of the Lorentz transformation. The six basis matrices $\mathcal{M}^{\rho\sigma}$ are called the *generators* of the Lorentz transformations. Crucially, these generators obey the Lie algebra relations of the Lorentz group

$$[\mathcal{M}^{\rho\sigma}, \mathcal{M}^{\tau\nu}] = \eta^{\sigma\tau}\mathcal{M}^{\rho\nu} - \eta^{\rho\tau}\mathcal{M}^{\sigma\nu} + \eta^{\rho\nu}\mathcal{M}^{\sigma\tau} - \eta^{\sigma\nu}\mathcal{M}^{\rho\tau} \tag{1.26}$$

A finite Lorentz transformation can be expressed as the exponential

$$\Lambda = \exp\left(\frac{1}{2}\Omega_{\rho\sigma}\mathcal{M}^{\rho\sigma}\right) \tag{1.27}$$

1.3.3 The Spinor Representation

In order to find other matrices which satisfy the Lorentz Lie algebra conditions, the spinor representation is constructed. To do this, we must find matrices γ^μ, with $\mu = 0, 1, 2, 3$ such that it satisfies the following *Clifford algebra*

$$\{\gamma^\mu, \gamma^\nu\} \equiv \gamma^\mu\gamma^\nu + \gamma^\nu\gamma^\mu = 2\eta^{\mu\nu} \tag{1.28}$$

We can construct many other representations of the Clifford algebra by taking $V\gamma^\mu V^{-1}$ for any invertible matrix V. Of course, the main point of consideration is the relationship between the Clifford algebra and the Lorentz group. Let us define

$$S^{\rho\sigma} = \frac{1}{4}[\gamma^\rho, \gamma^\sigma] = \begin{cases} 0 & \rho = \sigma \\ \frac{1}{2}\gamma^\rho\gamma\sigma & \rho \neq \sigma \end{cases} = \frac{1}{2}\gamma^\rho\gamma^\sigma - \frac{1}{2}\eta^{\rho\sigma} \tag{1.29}$$

From this, we can prove that the matrices $S^{\mu\nu}$ form a representation of the Lorentz Lie algebra

$$[S^{\mu\nu}, S^{\rho\sigma}] = \eta^{\nu\rho}S^{\mu\sigma} - \eta^{\mu\rho}S^{\nu\sigma} + \eta^{\mu\sigma}S^{\nu\rho} - \eta^{\nu\sigma}S^{\mu\rho} \tag{1.30}$$

When $\mu \neq \nu$, we have

$$\begin{aligned}
[S^{\mu\nu}, \gamma^\rho] &= \frac{1}{2}[\gamma^\mu\gamma^\nu, , \gamma^\rho] \\
&= \frac{1}{2}\gamma^\mu\gamma^\nu, \gamma^\rho - \frac{1}{2}\gamma^\rho\gamma^\mu, \gamma^\nu \\
&= \frac{1}{2}\gamma^\mu\{\gamma^\nu, \gamma^\rho\} - \frac{1}{2}\gamma^\mu\gamma^\nu\gamma^\rho - \frac{1}{2}\gamma^\rho\gamma^\mu\gamma^\nu + \frac{1}{2}\gamma^\mu\gamma^\nu\gamma^\rho \\
&= \gamma^\mu\eta^{\nu\rho} - \gamma^v\eta^{\rho\mu}
\end{aligned}$$

Taking $\rho \neq \sigma$ and using the above result

$$\begin{aligned}
[S^{\mu\nu}, S^{\rho\sigma}] &= \frac{1}{2}[S^{\mu\nu}, \gamma^\rho\gamma^\sigma] \\
&= \frac{1}{2}[S^{\mu\nu}, \gamma^\rho] + \frac{1}{2}\gamma^\rho[S^{\mu\nu}, \gamma^\sigma] \\
&= \frac{1}{2}\gamma^\mu\gamma^\sigma\eta^{\nu\rho} - \frac{1}{2}\gamma^\nu\gamma^\sigma\eta^{\nu\mu} + \frac{1}{2}\gamma^\rho\gamma^\mu\eta^{\nu\sigma} - \frac{1}{2}\gamma^\rho\gamma^\nu\eta^{\sigma\mu}
\end{aligned}$$

Now substituting the expression $\gamma^\mu\gamma^\sigma = 2S^{\mu\sigma} + \eta^{\mu\sigma}$, we obtain,

$$[S^{\mu\nu}, S^{\rho\sigma}] = S^{\mu\sigma}\eta^{\nu\rho} - S^{\nu\sigma}\eta^{\rho\mu} + S^{\rho\mu}\eta^{\nu\sigma} - S^{\rho\nu}\eta^{\sigma\mu} \tag{1.31}$$

We construct a new field to work with, the Dirac spinor ψ. The Dirac spinor field $\psi^\alpha(x)$ is an object with four complex components labelled by $\alpha = 1, 2, 3, 4$ in 3+1 dimensions. The field was introduced so that it could be acted upon by the matrices $(S^{\mu\nu})^\alpha{}_\beta$. The $S^{\mu\nu}$ matrices are 4×4 since the γ^μ matrices are 4×4 in 3+1 dimensions. Under Lorentz transformations, we obtain

$$\psi^\alpha(x) \to S[\Lambda]^\alpha{}_\beta \psi^\beta(\Lambda^{-1}x) \tag{1.32}$$

where

$$\Lambda = \exp\left(\frac{1}{2}\Omega_{\rho\sigma}\mathcal{M}^{\rho\sigma}\right) \tag{1.33}$$

$$S[\Lambda] = \exp\left(\frac{1}{2}\Omega_{\rho\sigma}S^{\rho\sigma}\right) \tag{1.34}$$

Since the same six numbers $\Omega_{\rho\sigma}$ are in both Λ and $S[\Lambda]$, the same Lorentz transformation is on x and ψ, even although the basis of generators of $\mathcal{M}^{\rho\sigma}$ and $S^{\rho\sigma}$ are different.

1.3.4 The Dirac Action S

From the new Dirac spinor field ψ, we can construct a Lorentz invariant equation of motion, from a Lorentz invariant action. Let us define the *Dirac adjoint* where

$$\bar{\psi}(x) = \psi^\dagger(x)\gamma^0 \tag{1.35}$$

Using this, we can prove that $\bar{\psi}\psi$ is a Lorentz scalar.

Under a Lorentz transformation

$$\begin{aligned}\bar{\psi}(x)\psi(x) &= \psi^\dagger(x)\gamma^0\psi(x)\\ &\to \psi^\dagger(\Lambda^{-1}x)S[\Lambda]^\dagger\gamma^0 S[\Lambda]\psi(\Lambda^{-1})\\ &= \psi^\dagger(\Lambda^{-1}x)\gamma^0\psi(\Lambda^{-1})\\ &= \bar{\psi}(\Lambda^{-1}x)\psi(\Lambda^{-1}x)\end{aligned} \tag{1.36}$$

which is clearly the transformation law for a Lorentz scalar. We can also prove that $\bar{\psi}\gamma^\mu\psi$ is a Lorentz vector as follows

Under a Lorentz transformation, we have

$$\bar{\psi}S[\Lambda]^{-1}\gamma^\mu S[\Lambda]\psi \tag{1.37}$$

In order to transform as a vector, we must have

$$S[\Lambda]^{-1}\gamma^\mu S[\Lambda] = \Lambda^\mu{}_\nu\gamma^\mu \tag{1.38}$$

Working infinitesimally

$$\Lambda = \exp\left(\frac{1}{2}\Omega_{\rho\sigma}\rho\sigma\right) \approx 1 + \frac{1}{2}\Omega_{\rho\sigma}\mathcal{M}^{\rho\sigma} + \cdots \tag{1.39}$$

$$S[\Lambda] = \exp\left(\frac{1}{2}\Omega_{\rho\sigma}S^{\rho\sigma}\right) \approx 1 + \frac{1}{2}\Omega_{\rho\sigma}S^{\rho\sigma} + \cdots \tag{1.40}$$

$$-[S^{\rho\sigma}, \gamma^{\mu}] = (\mathcal{M}^{\rho\sigma})^{\mu}{}_{\nu}\gamma^{\nu} \tag{1.41}$$

Expanding out $\mathcal{M}$

$$\begin{aligned}(\mathcal{M}^{\rho\sigma})^{\mu}{}_{\nu}\gamma^{\mu} &= (\eta^{\rho\mu}\delta^{\sigma}_{\nu} - \eta^{\sigma\rho}\delta^{\mu}_{\nu})\gamma^{\nu} \\ &= \eta^{\rho}\gamma^{\mu\sigma} - \eta^{\sigma\mu}\gamma^{\rho}\end{aligned} \tag{1.42}$$

Thus the proof follows

$$[S^{\rho\sigma}, \gamma^{\mu}] = \eta^{\rho}\gamma^{\mu\sigma} - \eta^{\sigma\mu}\gamma^{\rho} \tag{1.43}$$

And similarly, we can also show that $\bar{\psi}\gamma^{\mu}\gamma^{\nu}\psi$ transforms as a Lorentz tensor. Finally having obtained three bilinears of the Dirac field, $\bar{\psi}\psi$, $\bar{\psi}\gamma^{\mu}\psi$ and $\bar{\psi}\gamma^{\mu}\gamma^{\nu}\psi$, each of which transforms covariantly under the Lorentz group, we can construct a Lorentz invariant action as follows

$$S = \int d^4x\, \bar{\psi}(x)\left(i\gamma^{\mu}\partial_{\mu} - m\right)\psi(x) \tag{1.44}$$

$$= \int d^4x\, \mathcal{L}(x) \tag{1.45}$$

This is defined as the *Dirac action*. From this, we can extract a first order Lagrangian, the *Dirac Lagrangian* $\mathcal{L}(x)$, defined as follows

$$\mathcal{L}(x) = \bar{\psi}(x)(i\gamma^{\mu}\partial_{\mu} - m)\psi(x) \tag{1.46}$$

For spinor fields, the nature of the γ^{μ} matrices means that the Dirac Lagrangian is Lorentz invariant, as desired.

1.3.5 The Dirac Equation

Using the Euler-Lagrange equation in Eq. (1.47), we can vary the Dirac Lagrangian, $\mathcal{L}$, with respect to ψ and $\bar{\psi}$ independently to obtain the equation of motion.

$$\frac{\partial\mathcal{L}}{\partial\psi} - \partial_{\mu}\frac{\partial\mathcal{L}}{\partial(\partial_{\mu}\psi)} = 0 \tag{1.47}$$

Varying with respect to ψ yields the *Dirac equation*

$$(i\gamma^{\mu}\partial_{\mu} - m)\psi = 0 \tag{1.48}$$

while varying with respect to $\bar{\psi}$ yields the conjugate equation

$$i\partial_{\mu}\bar{\psi}\gamma^{\mu} + m\bar{\psi} = 0 \tag{1.49}$$

Despite the Dirac equation being first order in derivatives, it is remarkably Lorentz invariant.

1.4 Dirac-Like theory in 3+1 Dimensions

A Dirac-like theory of fermions in 3+1 dimensions can be described by the same Hamiltonian form as Eq. (1.7)

$$H = \psi^\dagger \mathcal{H} \psi$$

where $\psi = (\psi_1, \psi, \ldots, \psi_n)^T$ is a n-component spinor where, in this case, n can be even or odd. This is in contrast to the Dirac case where $n = 2^s$. The density Hamiltonian $\mathcal{H}$ is written as the following

$$\mathcal{H} = \beta_i p_i + \beta_4 m_1 + \beta_5 m_2 \tag{1.50}$$

where m_1 and m_2 are two independent mass terms, $p_i = (p_x, p_y, p_z)$ are the momenta and $\beta_\mu = (\beta_x, \beta_y, \beta_z, \beta_4, \beta_5)$ are $n \times n$ matrices which do not satisfy the Clifford algebra $\mathrm{Cl}_{3,1}$

$$\implies \{\beta_\mu, \beta_\nu\} \equiv \beta_\mu \beta_\nu + \beta_\nu \beta_\mu \neq 2\delta_{\mu\nu} \mathbb{1} \tag{1.51}$$

where $\delta_{\mu\nu}$ is the Kronecker delta and $\mathbb{1}$ is the identity matrix. By diagonalising the density Hamiltonian $\mathcal{H}$, the following eigenvalues are obtained

$$\begin{aligned} E_0^j = 0, \quad E_{1,-}^k = -\sqrt{p_x^2 + p_y^2 + p_z^2 + {m_1}^2}, \quad E_{1,+}^k = \sqrt{p_x^2 + p_y^2 + p_z^2 + {m_1}^2} \\ E_{2,-}^l = -\sqrt{p_x^2 + p_y^2 + p_z^2 + {m_2}^2}, \quad E_{2,+}^l = \sqrt{p_x^2 + p_y^2 + p_z^2 + {m_2}^2} \end{aligned} \tag{1.52}$$

where j, k, l are degeneracy of the corresponding eigenvalues.

1.4.1 $SO(3)$ Symmetry of the Dirac-like Model

Our model follows $SO(3)$ symmetry. Consider (3+1)-dimensional spacetime, where the metric is flat, $g_{\mu\nu} = \eta_{\mu\nu}$. Then consider a field $\psi(x)$ on this spacetime which is a Lorentz scalar and where $x \in \mathbb{R}^{1,3}$ is a point on the spacetime. An assumption can be made that $\psi(x)$ is transformed by the integer spinor representation of $SO(3)$ gauge group. We can denote an explicit transformation $U(x) \in SO(3)$, where ψ undergoes transformation

$$\psi(x) \implies \psi^U(x) := S[U](x)\psi(x) \tag{1.53}$$

where $S[U]$ is the spin-s representation of $U(x) \in SO(3)$ and $s = 1, 2, 3, \ldots$ A Lagrangian $\mathcal{L}$ can be expressed which is invariant under this $SO(3)$ transformation

$$\mathcal{L} = \bar{\psi} i \gamma^\mu \partial_\mu \psi \tag{1.54}$$

The Lie algebra for $SO(3)$ for dimension n is

$$so(3) := \left\{ X : n \times n \text{ matrix } | X^T + X = 0, \mathrm{Tr}(X) = 0 \right\} \tag{1.55}$$

For any component $U \in SO(3)$, it can be expanded as

$$U = \exp(iaJ_1 + ibJ_2 + icJ_3) \tag{1.56}$$

where J_1, J_2, J_3 are the generators of this algebra and obey the following commutation relation

$$[J_i, J_j] = J_k \delta_{ij} \tag{1.57}$$

For each value of n we consider, it corresponds to different spin, $s \Longrightarrow 2s{+}1 = n$. Now, we can define a field ψ_s which undergoes a transformation by spin-s representation of $SO(3)$, where $s = 1, 2, 3, \ldots$.

$$\psi_s = (\psi_1, \cdots, \psi_{2^{s-1}}) \tag{1.58}$$

where ψ_j are fields transformed as spin-1/2 representation of SO(3) group. Thus, we can obtain ψ_s as a 2^s component field.

1.4.2 Non-Lorentz Invariance of Dirac-Like Model

A key distinction of our Dirac-like model is that it is not Lorentz invariant. This is due to the result of having at least one zero eigenvalue, $E = 0$, from the density Hamiltonian $\mathcal{H}$. Consider two inertial frames of reference, S and S'. Since energy E is not Lorentz invariant, if we measure the energy of the system in S to be zero, then it follows from the relativistic kinematic expression that

$$E_S = \sqrt{|p|^2c^2 + m^2c^4} \equiv c\sqrt{|p|^2 + m^2c^2} = 0 \tag{1.59}$$

For fields with non-superluminal speeds, there exists only two possibilities in frame S:

1. Both momentum $|p|$ and mass m are zero.
2. $c = 0$

Now consider the new frame S', where a Lorentz transformation yields that the measured energy of the system now is not zero, $E_{S'} \neq 0$

$$E_{S'} = c\sqrt{|p|^2 + m^2c^2} \neq 0 \tag{1.60}$$

By examining 1., it is clear that this is a trivial case. There is no description of a tangible system since both the mass m and momentum $|p|$ are zero. Thus the only other possibility is that $c = 0$. However, from the postulates of special relativity, the speed of light c must be the same in all inertial frames of reference. Since we have taken $c = 0$ in frame S, then it should hold for frame S'. This leads to $E_{S'} = 0$, which is an explicit contradiction of the case in Eq. (1.60). Thus, a clear violation of special relativity can be seen, meaning that our Dirac-like model cannot describe

relativistic particles.

This is not necessarily problematic since the natural application of these Dirac-like fermions are generally found in low energy condensed matter systems. As recalled previously, fermions in these systems are not constrained by Poincaré symmetry, the full symmetry of special relativity. For instance, in conventional crystals, they are rather constrained by the crystal symmetry of the 230 space groups of the 3D lattices. This leads to possible exotic free fermionic quasiparticles with no counterpart in high energy physics. However, experimental evidence dictates that the relativistic energy expressions from the eigenvalues are required, which are used to describe the real spectra of the energy dispersion relations $E(k)$ of these exotic fermion types.

Chapter 2

Method

The main goals of the project are outlined as follows:

1. Construct $n \times n$ matrices $\beta_\mu = (\beta_x, \beta_y, \beta_z, \beta_4, \beta_5)$ for $5 \leq n \leq 8$ such that the corresponding Hamiltonian has the desired eigenvalues in Eqs. (1.52).
2. Plot the real spectra of energy dispersion relations $E(k)$ for $5 \leq n \leq 8$.
3. Identify possible β_6 associated with a third independent mass term m_3.

The primary method to achieve this objective involves using the computational software program Wolfram Mathematica. With this, we construct the $n \times n$ matrices and from there, we can straightforwardly decompose the matrix into the five β_μ matrix components. The overall method of construction was governed by an attitude of brute force, through rigorous trial and error. These eigenvalues would then be plotted to illustrate the real spectra of energy dispersion relations $E(k)$ for each n.

The search for β_6, giving rise to m_3, allows us to construct a possible Dirac-like density Hamiltonian $\mathcal{H}$ as shown

$$\mathcal{H} = \beta_i p_i + \beta_4 m_1 + \beta_5 m_2 + \beta_6 m_3 \tag{2.1}$$

2.0.1 Characteristic Polynomial

The initial stages of the method involved analysing the form of the resulting characteristic polynomial that would yield the desired eigenvalues of Eqs. (1.52). If we consider a matrix A, the eigenvalues of A are solutions to the characteristic equation

$$|A - \lambda \mathbb{1}| = 0 \tag{2.2}$$

Taking the simplest case, which is $n = 5$, the characteristic equation must factorise to

$$\lambda(\lambda^2 - p_x^2 - p_y^2 - p_z^2 - m_1^2)(\lambda^2 - p_x^2 - p_y^2 - p_z^2 - m_2^2) = 0 \tag{2.3}$$

By expanding this quintic expression, we obtain

$$\lambda^5 + \lambda^3\left(-2p_x^2 - 2p_y^2 - 2p_z^2 - m_1^2 - m_2^2\right) + \lambda\big(p_x^4 + p_y^4 + p_z^4 + 2p_x^2p_y^2 + 2p_x^2p_z^2 + 2p_y^2p_z^2 + p_x^2m_1^2 + p_y^2m_1^2 + p_y^2m_1^2 + p_x^2m_2^2 + p_y^2m_2^2 + p_z^2m_2^2 + m_1^2m_2^2\big)$$

Our approach was to study the coefficients of each power of λ. Through rigorous trial and error, we aimed to determine a form for the 5×5 matrix, such that the even powers of λ would be eliminated. Eventually, we were able to construct a 5×5 matrix that yielded the correct coefficient for λ^3. However, this 'pen and paper' approach proved practically futile to obtain the linear term and, as a result, it was discarded. Another approach had to be considered.

2.0.2 Gell-Mann Matrices

Our supervisor Gian introduced us to the Gell-Mann matrices, which are a set of eight linearly independent 3×3 Hermitian matrices, used in the study of the strong interaction in particle physics, especially the color quantum number of the gluon fields. The important property of these Gell-Mann matrices is that they do not satisfy the Clifford algebra $\mathrm{Cl}_{3,1} \implies \{\lambda_i, \lambda_j\} \neq 2\delta_{ij}\mathbb{1}$. There are four Gell-Mann matrices of interest

$$\lambda_1 = \begin{bmatrix} 0 & 1 & 0 \\ 1 & 0 & 0 \\ 0 & 0 & 0 \end{bmatrix} \qquad \lambda_2 = \begin{bmatrix} 0 & i & 0 \\ -i & 0 & 0 \\ 0 & 0 & 0 \end{bmatrix}$$
$$\lambda_6 = \begin{bmatrix} 0 & 0 & 0 \\ 0 & 0 & 1 \\ 0 & 1 & 0 \end{bmatrix} \qquad \lambda_7 = \begin{bmatrix} 0 & 0 & 0 \\ 0 & 0 & i \\ 0 & -i & 0 \end{bmatrix} \tag{2.4}$$

It proved satisfactory since by incorporating the Gell-Mann matrices into the expression for the Dirac density Hamiltonian $\mathcal{H}$ in Eq. (1.8)

$$\mathcal{H} = \lambda_1 p_x + \lambda_2 p_y + \lambda_6 p_z + \lambda_7 m \tag{2.5}$$

we obtain the following matrix

$$\mathcal{H} = \begin{bmatrix} 0 & p_x + ip_y & 0 \\ p_x - ip_y & 0 & p_z + im \\ 0 & p_z - im & 0 \end{bmatrix} \tag{2.6}$$

yielding the desired Dirac-like eigenvalues in Eqs. (1.52),

$$E_0^1 = 0, \qquad E_{1,-}^1 = -\sqrt{p_x^2 + p_y^2 + p_z^2 + {m_1}^2}, \qquad E_{1,+}^1 = \sqrt{p_x^2 + p_y^2 + p_z^2 + {m_1}^2} \tag{2.7}$$

where the superscript denotes the degeneracy of the corresponding eigenvalues.

From this, we considered that the next approach should, to some degree, incorporate these matrices or their matrix elements for the construction of the β_μ matrices. The standard matrix elements in our desired configurations would consist of a real component and an imaginary component, corresponding to a mass term or a momenta term. Additional mass terms can also be constructed from two mass terms as mentioned in Sect.(2.0.4).

2.0.3 Direct Sum

The crucial distinction of the Dirac-like model is the inclusion of a second independent mass term m_2. At this point, there are two known matrices that yielded the desired eigenvalues of Eqs. (1.52), the Dirac density Hamiltonian and the density Hamiltonian constructed from the Gell-Mann matrices $\lambda_{i=1,2,6,7}$. Our intuitive procedure was to utilise and combine these matrices to construct $n \times n$ matrices for $n = 5, 6, 7, 8$. A tensor product would be one method of combination, but cannot be considered since this would result in the emergence of cross terms such as between m_1 and m_2. The mass terms of the Dirac-like model must be independent. So a direct sum was considered, which ensured no mixing between the rows and columns of the two submatrices, which would each correspond to a mass term, m_1 or m_2. The following example of the direct sum is given for the 6×6 case with two Gell-Mann density Hamiltonian submatrices

$$\mathcal{H}_{n=6} = \begin{bmatrix} 0 & p_x + ip_y & 0 & 0 & 0 & 0 \\ p_x - ip_y & 0 & pz + im_1 & 0 & 0 & 0 \\ 0 & p_z - im_1 & 0 & 0 & 0 & 0 \\ 0 & 0 & 0 & 0 & p_x + ip_y & 0 \\ 0 & 0 & 0 & p_x - ip_y & 0 & p_z + im_2 \\ 0 & 0 & 0 & 0 & p_z - im_2 & 0 \end{bmatrix} \tag{2.8}$$

which yielded the following eigenvalues

$$\begin{aligned} E_0^2 = 0, \quad E_{1,-}^1 = -\sqrt{p_x^2 + p_y^2 + p_z^2 + {m_1}^2}, \quad E_{1,+}^1 = \sqrt{p_x^2 + p_y^2 + p_z^2 + {m_1}^2} \\ E_{2,-}^1 = -\sqrt{p_x^2 + p_y^2 + p_z^2 + {m_2}^2}, \quad E_{2,+}^1 = \sqrt{p_x^2 + p_y^2 + p_z^2 + {m_2}^2} \end{aligned} \tag{2.9}$$

in agreement with the desired Dirac-like eigenvalues of Eqs. (1.52).

The most problematic case to address was the 5×5, as this was the only case where the direct sum approach supposedly failed, at least one cross term always emerged. Also, the direct sum approach felt trivial to use since it worked for a low number of specific cases, where the independent masses were separated.

2.0.4 Grouping Of Mass Terms

From experimenting with the terms of both the Gell-Mann and Dirac Hamiltonian densities, and with the direct sum approach, we obtained a number of Hamiltonian configurations which produced eigenvalues of the following form

$$E = \sqrt{p_x^2 + p_y^2 + p_z^2 + m_1^2 + m_2^2 + \cdots + m_n^2} \tag{2.10}$$

This form appeared quite often in our search for appropriate β_μ matrices, which we previously discarded since the mass terms appear in the same eigenvalue.

However, an absolutely crucial point to consider is that you can group the mass terms with sufficient free parameters into a single mass term, which we can effectively treat as independent. We can take $m_1^2 + m_2^2 + \cdots + m_n^2 = M^2$, thus obtaining a mass term M. Since we can treat, for instance, m_1 and M as independent mass terms, this satisfies our Dirac-like model.

2.0.5 Spin-s Representation of $SO(3)$

The following general procedure was applied to construct the spin-s representation of $SO(3)$. An explicit case of 5×5 is written as a following example.

The dimensionality of the spin-s representation is $2s + 1$, thus for the 5×5 case

$$2s + 1 = 5 \Longrightarrow s = 2 \tag{2.11}$$

We consider the standard choice of z-axis but since there is nothing special about it from a basis perspective, we look for a representation in arbitrary oriented axes. The values of the spin projections, σ, are

$$\sigma = \hbar\,(s,\ s-1, \cdots,\ -s+1,\ -s) \Longrightarrow \{2\hbar,\ \hbar,\ 0,\ -\hbar,\ -2\hbar\} \tag{2.12}$$

We obtain $\hat{S}_z$ which is diagonal in its own basis

$$\left\{\hat{S}_z\right\}_{\sigma'\sigma} = \langle s, \sigma'|\, \hat{S}_z\, |s, \sigma\rangle = \hbar\, diag(s,\ s-1, \cdots,\ -s+1,\ -s) \tag{2.13}$$

Writing as a full matrix

$$\langle \sigma'|\, \hat{S}_z\, |\sigma\rangle = \hbar \begin{bmatrix} 2 & 0 & 0 & 0 & 0 \\ 0 & 1 & 0 & 0 & 0 \\ 0 & 0 & 0 & 0 & 0 \\ 0 & 0 & 0 & -1 & 0 \\ 0 & 0 & 0 & 0 & -2 \end{bmatrix} \tag{2.14}$$

Using the well known ladder operators

$$\hat{S}_{\pm} = \hat{S}_x \pm i\hat{S}_y \tag{2.15}$$

we obtain the relations

$$\hat{S}_x = \frac{1}{2}(\hat{S}_+ + \hat{S}_-) \qquad \hat{S}_y = -\frac{i}{2}(\hat{S}_+ - \hat{S}_-) \tag{2.16}$$

Following the action of these ladder operators on our basis vectors

$$\hat{S}_{\pm} |s, \sigma\rangle = \hbar c^{\pm}_{s,\sigma} |s, \sigma + 1\rangle \qquad c^{\pm}_{s,\sigma} = \sqrt{(s \mp \sigma)(s \pm \sigma + 1)} \tag{2.17}$$

Writing explicitly for the 5×5 case

$$c^{+}_{2,\sigma} = \left\{0, 2, \sqrt{6}, \sqrt{6}, 2\right\} \tag{2.18}$$

$$c^{-}_{2,\sigma} = \left\{2, \sqrt{6}, \sqrt{6}, 2, 0\right\} \tag{2.19}$$

Hence the matrix representations of $\hat{S}_+$ and its Hermitian conjugate $\hat{S}_-$ are

$$\langle\sigma'| \hat{S}_+ |\sigma\rangle = \hbar \begin{bmatrix} 0 & 2 & 0 & 0 & 0 \\ 0 & 0 & \sqrt{6} & 0 & 0 \\ 0 & 0 & 0 & \sqrt{6} & 0 \\ 0 & 0 & 0 & 0 & 2 \\ 0 & 0 & 0 & 0 & 0 \end{bmatrix} \qquad \langle\sigma'| \hat{S}_- |\sigma\rangle = \hbar \begin{bmatrix} 0 & 0 & 0 & 0 & 0 \\ 2 & 0 & 0 & 0 & 0 \\ 0 & \sqrt{6} & 0 & 0 & 0 \\ 0 & 0 & \sqrt{6} & 0 & 0 \\ 0 & 0 & 0 & 2 & 0 \end{bmatrix} \tag{2.20}$$

Using Eqs. (2.16), we find

$$\langle\sigma'| \hat{S}_x |\sigma\rangle = \frac{\hbar}{2} \begin{bmatrix} 0 & 2 & 0 & 0 & 0 \\ 2 & 0 & \sqrt{6} & 0 & 0 \\ 0 & \sqrt{6} & 0 & \sqrt{6} & 0 \\ 0 & 0 & \sqrt{6} & 0 & 2 \\ 0 & 0 & 0 & 2 & 0 \end{bmatrix} \qquad \langle\sigma'| \hat{S}_y |\sigma\rangle = \frac{i\hbar}{2} \begin{bmatrix} 0 & -2 & 0 & 0 & 0 \\ 2 & 0 & -\sqrt{6} & 0 & 0 \\ 0 & \sqrt{6} & 0 & -\sqrt{6} & 0 \\ 0 & 0 & \sqrt{6} & 0 & -2 \\ 0 & 0 & 0 & 2 & 0 \end{bmatrix} \tag{2.21}$$

From this, we have obtained the spin-2 representation for $SO(3)$ for the explicit 5×5 case. This general procedure was applied to the higher n-dimensional matrices for $5 \leq n \leq 8$. The generators, S_i, for each spin-s representation should satisfy the following commutation relation

$$[S_i, S_j] = \delta_{ij} S_k \qquad i, j, k = x, y, z \tag{2.22}$$

Chapter 3

Results

3.1 5×5 Case

For the 5×5 case, the first successful matrix obtained was proposed by our supervisor Gian. Our initial procedure to finding appropriate matrices, yielding the desired eigenvalues of Eqs. (1.52), was with the direct sum approach. It worked for all cases, except 5×5, since at least one cross-term always emerged. The first successful matrix is as follows

$$\mathcal{H}_{n=5} = \begin{bmatrix} 0 & p_x + im_1 & -m_2 + im_3 & 0 & ip_y - p_z \\ p_x - im_1 & 0 & 0 & ip_y - p_z & 0 \\ -m_2 - im_3 & 0 & 0 & im_4 + m_5 & 0 \\ 0 & -ip_y - p_z & -im_4 + m_5 & 0 & -p_x + im_1 \\ -ip_y - pz & 0 & 0 & -p_x - im_1 & 0 \end{bmatrix} \tag{3.1}$$

which yielded the following eigenvalues

$$E = 0,\, 0,\, \pm\sqrt{p_x^2 + p_y^2 + p_z^2 + {m_1}^2},\, \pm\sqrt{p_x^2 + p_y^2 + p_z^2 + {m_1}^2 + {m_2}^2 + {m_3}^2 + {m_4}^2 + {m_5}^2} \tag{3.2}$$

As outlined in Sect.(2.0.4), the grouping of the mass terms with sufficient free parameters, means we can express

$${m_1}^2 + {m_2}^2 + {m_3}^2 + {m_4}^2 + {m_5}^2 = M^2 \tag{3.3}$$

which yields the resulting eigenvalues

$$\begin{aligned} E_0^2 = 0, \qquad E_{1,-}^1 &= -\sqrt{p_x^2 + p_y^2 + p_z^2 + {m_1}^2}, \qquad E_{1,+}^1 = \sqrt{p_x^2 + p_y^2 + p_z^2 + {m_1}^2} \\ E_{2,-}^1 &= -\sqrt{p_x^2 + p_y^2 + p_z^2 + M^2}, \qquad E_{2,+}^l = \sqrt{p_x^2 + p_y^2 + p_z^2 + M^2} \end{aligned} \tag{3.4}$$

where the superscript denotes the degeneracies and m_1, M can act as independent mass terms, satisfying our Dirac-like model.

3.1.1 Non-Hermitian Density Hamiltonian $\mathcal{H}_{n=5}$?

From experimentation with the previous matrix (3.1), we encountered an unexpected result. We managed to construct the following density Hamiltonian

$$\mathcal{H}_{n=5} = \begin{bmatrix} 0 & p_x + im_1 & m_2 & 0 & ip_y - p_z \\ p_x - im_1 & 0 & 0 & ip_y - p_z & 0 \\ m_2 & 0 & 0 & m_1 & 0 \\ 0 & -ip_y - p_z & -m_1 & 0 & -p_x + im_1 \\ -ip_y - pz & 0 & 0 & -p_x - im_1 & 0 \end{bmatrix} \tag{3.5}$$

which produced the following eigenvalues

$$\begin{aligned} E_0^2 = 0, \quad E_{1,-}^1 = -\sqrt{p_x^2 + p_y^2 + p_z^2 + {m_1}^2}, \quad E_{1,+}^1 = \sqrt{p_x^2 + p_y^2 + p_z^2 + {m_1}^2} \\ E_{2,-}^1 = -\sqrt{p_x^2 + p_y^2 + p_z^2 + {m_2}^2}, \quad E_{2,+}^1 = \sqrt{p_x^2 + p_y^2 + p_z^2 + {m_2}^2} \end{aligned} \tag{3.6}$$

where the superscript denotes the degeneracy of the corresponding eigenvalues.

This is an interesting case to consider, which was not part of our original investigation. The 5×5 matrix $\mathcal{H}_{n=5}$ in (3.5) is clearly not Hermitian, yet the eigenvalues are real, describing a real spectrum of energy dispersion relations, $E(k)$. This result sparks an unprecedented interest and research into non-Hermitian quantum mechanics, which includes specific systems such as parity-time ($\mathcal{PT}$) symmetry. In this case, the Hamiltonian density $\mathcal{H}_{n=5}$ can be classified as *pseudo-Hermitian*. Mostafazadeh [4] mentioned that a non-Hermitian Hamiltonian with a real spectrum can be referred to as pseudo-Hermitian.

3.1.2 5×5 Spin-s Representation of $SO(3)$

The entire procedure for the resulting representation of $SO(3)$ is outlined in Sect.(2.0.5), which explicitly gives the 5×5 case as an example. However, just to reiterate

$$\langle \sigma' | \hat{S}_x | \sigma \rangle = \frac{\hbar}{2} \begin{bmatrix} 0 & 2 & 0 & 0 & 0 \\ 2 & 0 & \sqrt{6} & 0 & 0 \\ 0 & \sqrt{6} & 0 & \sqrt{6} & 0 \\ 0 & 0 & \sqrt{6} & 0 & 2 \\ 0 & 0 & 0 & 2 & 0 \end{bmatrix} \qquad \langle \sigma' | \hat{S}_y | \sigma \rangle = \frac{i\hbar}{2} \begin{bmatrix} 0 & -2 & 0 & 0 & 0 \\ 2 & 0 & -\sqrt{6} & 0 & 0 \\ 0 & \sqrt{6} & 0 & -\sqrt{6} & 0 \\ 0 & 0 & \sqrt{6} & 0 & -2 \\ 0 & 0 & 0 & 2 & 0 \end{bmatrix}$$

$$\langle \sigma' | \hat{S}_z | \sigma \rangle = \hbar \begin{bmatrix} 2 & 0 & 0 & 0 & 0 \\ 0 & 1 & 0 & 0 & 0 \\ 0 & 0 & 0 & 0 & 0 \\ 0 & 0 & 0 & -1 & 0 \\ 0 & 0 & 0 & 0 & -2 \end{bmatrix}$$

The dimensionality of the spin-s representation is $2s+1$, thus for the 5×5 case

$$2s+1=5 \Longrightarrow s=2$$

From the 5×5 case, we have explicitly obtained the spin-2 representation for $SO(3)$.

3.1.3 5×5 Real Spectra of Energy Dispersion Relations $E(k)$

Naturally, we switch notation from momentum p to the standard crystal momentum k for energy dispersion relations $E(k)$ in condensed matter physics.

Using the eigenvalues in Eqs. (3.4), we plotted $E(k)$ for the 5×5 case using Wolfram Mathematica as shown

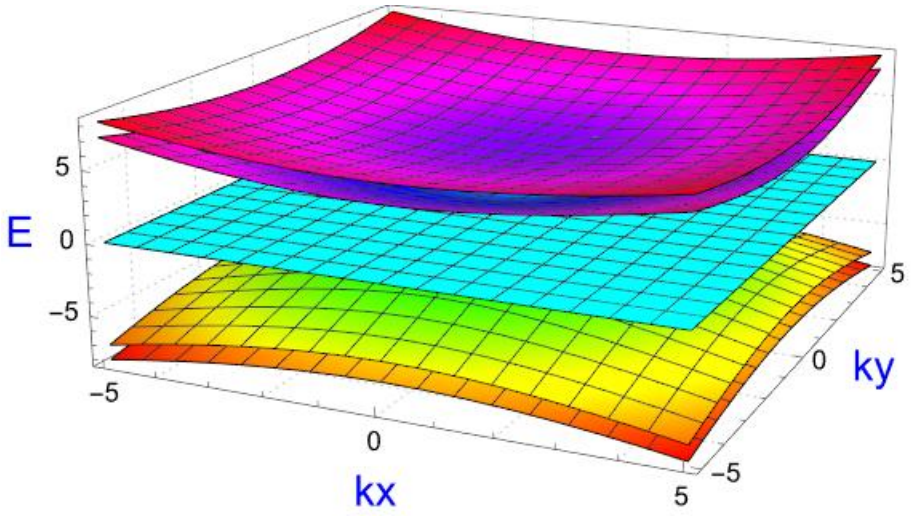

Figure 3.1: The 5×5 real spectra of energy dispersion relations $E(k)$ where $m_1 \neq M$.

The side view of the real spectra is also plotted in order to explicitly see the separation between the energy dispersion relations $E(k)$.

This resembles the energy dispersion $E(k)$ of A near a threefold degeneracy of exotic fermion types in SGs 199 and 214 in Fig (1.2), as illustrated in [2].

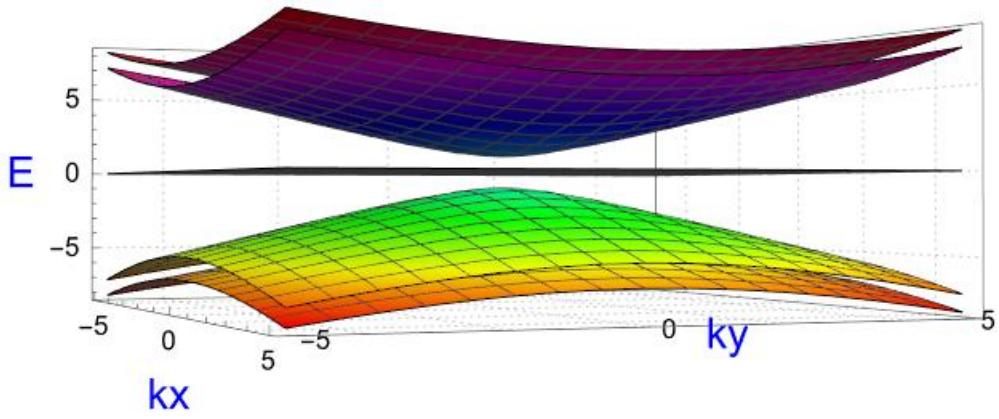

Figure 3.2: Side view of the 5×5 real spectra of energy dispersion relations $E(k)$ where $m_1 \neq M$.

3.1.4 Real Spectra of the 5×5 Non-Hermitian Density Hamiltonian $\mathcal{H}_{n=5}$

As previously mentioned in Sect.(3.1.1), a surprising case occurred whereby a non-Hermitian density Hamiltonian $\mathcal{H}_{n=5}$ was obtained, yielding eigenvalues which describe real spectra of the energy dispersion relations $E(k)$. This can be explicitly seen in the following illustration

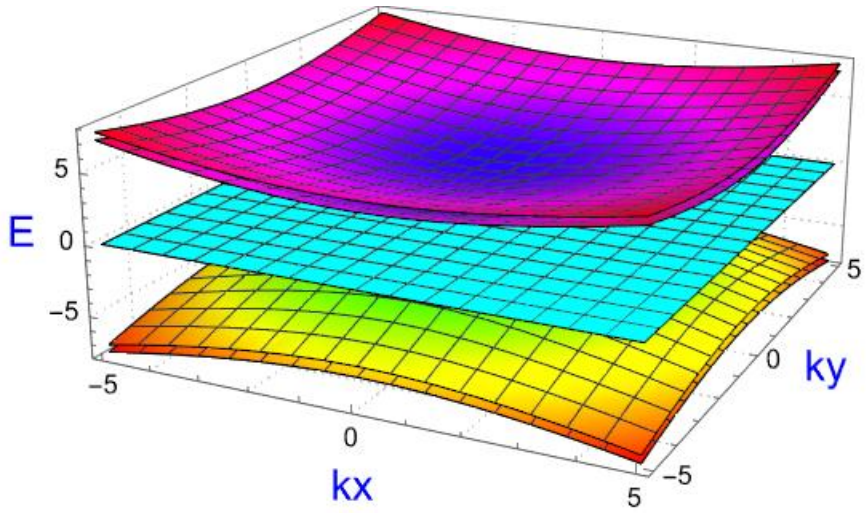

Figure 3.3: The real spectra of energy dispersion relations $E(k)$ for the non-Hermitian density Hamiltonian $\mathcal{H}_{n=5}$, where $m_1 \neq m_2$

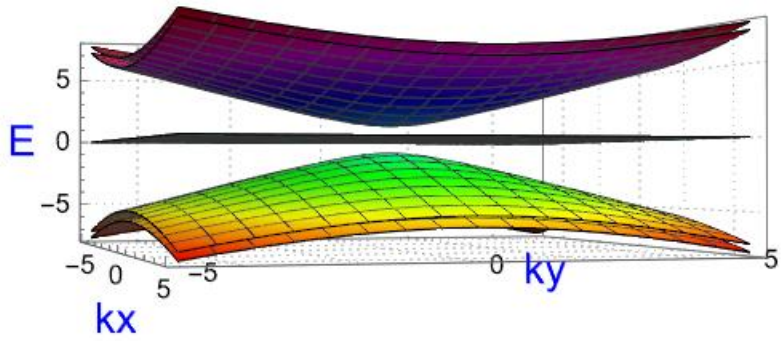

Figure 3.4: Side view of the real spectra of energy dispersion relations $E(k)$ for the non-Hermitian density Hamiltonian $\mathcal{H}_{n=5}$, where $m_1 \neq m_2$.

3.2 6×6 Case

The initial stages of the 6×6 case were predominantly influenced by the Gell-Mann matrices. We produced a straightforward result from the direct sum of two Gell-Mann Hamiltonian densities, corresponding to the two independent mass terms m_1 and m_2. This is outlined in Sect.(2.0.3) as an explicit example, but just to reiterate

$$\mathcal{H}_{n=6} = \begin{bmatrix} 0 & p_x + ip_y & 0 & 0 & 0 & 0 \\ p_x - ip_y & 0 & pz + im_1 & 0 & 0 & 0 \\ 0 & p_z - im_1 & 0 & 0 & 0 & 0 \\ 0 & 0 & 0 & 0 & p_x + ip_y & 0 \\ 0 & 0 & 0 & p_x - ip_y & 0 & p_z + im_2 \\ 0 & 0 & 0 & 0 & p_z - im_2 & 0 \end{bmatrix}$$

which yielded the following Dirac-like eigenvalues in Eqs. (1.52)

$$E_0^2 = 0, \quad E_{1,-}^1 = -\sqrt{p_x^2 + p_y^2 + p_z^2 + {m_1}^2}, \quad E_{1,+}^1 = \sqrt{p_x^2 + p_y^2 + p_z^2 + {m_1}^2}$$
$$E_{2,-}^1 = -\sqrt{p_x^2 + p_y^2 + p_z^2 + {m_2}^2}, \quad E_{2,+}^1 = \sqrt{p_x^2 + p_y^2 + p_z^2 + {m_2}^2}$$

where the superscript denotes the degeneracy of the corresponding eigenvalues. A number of matrices were constructed simply by rearrangement of these terms, but still direct sum was used.

Furthermore, Gian proposed a 6×6 example that did not utilise the direct sum

approach, with some degree of similarity to the 5×5 example of matrix (3.1)

$$\mathcal{H}_{n=6} = \begin{bmatrix} 0 & p_x + im_1 & im_2 - p_y & 0 & 0 & im_3 - p_z \\ p_x - im_1 & 0 & 0 & 0 & 0 & 0 \\ -im_2 - py & 0 & 0 & im_3 - p_z & 0 & 0 \\ 0 & 0 & -im_3 - p_z & 0 & -p_x & im_2 + p_y \\ 0 & 0 & 0 & -p_x & 0 & 0 \\ -im_3 - pz & 0 & 0 & -im_2 + p_y & 0 & 0 \end{bmatrix} \tag{3.7}$$

which produced the following eigenvalues

$$E = 0,\, 0,\, \pm\sqrt{p_x^2 + p_y^2 + p_z^2 + {m_2}^2 + {m_3}^2},\, \pm\sqrt{p_x^2 + p_y^2 + p_z^2 + {m_1}^2 + {m_2}^2 + {m_3}^2} \tag{3.8}$$

By manipulating his matrix example, we were able to construct a number of configurations, which includes the following

$$\mathcal{H}_{n=6} = \begin{bmatrix} 0 & p_x + im_1 & m_2 + im_3 & m_4 + im_5 & 0 & ip_y - p_z \\ p_x - im_1 & 0 & 0 & 0 & ip_y - p_z & 0 \\ m_2 - im_3 & 0 & 0 & 0 & 0 & 0 \\ m_4 - im_5 & 0 & 0 & 0 & 0 & 0 \\ 0 & -ip_y - p_z & 0 & 0 & 0 & -p_x + im_1 \\ -ip_y - p_z & 0 & 0 & 0 & -p_x - im_1 & 0 \end{bmatrix} \tag{3.9}$$

which yielded the following eigenvalues

$$E = 0,\, 0,\, \pm\sqrt{p_x^2 + p_y^2 + p_z^2 + {m_1}^2},\, \pm\sqrt{p_x^2 + p_y^2 + p_z^2 + {m_1}^2 + {m_2}^2 + {m_3}^2 + {m_4}^2 + {m_5}^2} \tag{3.10}$$

As outlined in Sect.(2.0.4), the grouping of the mass terms with sufficient free parameters, means we can express

$${m_1}^2 + {m_2}^2 + {m_3}^2 + {m_4}^2 + {m_5}^2 = M^2 \tag{3.11}$$

which yields the resulting eigenvalues

$$\begin{aligned} E_0^2 = 0, \qquad E_{1,-}^1 &= -\sqrt{p_x^2 + p_y^2 + p_z^2 + {m_1}^2}, \qquad E_{1,+}^1 = \sqrt{p_x^2 + p_y^2 + p_z^2 + {m_1}^2} \\ E_{2,-}^1 &= -\sqrt{p_x^2 + p_y^2 + p_z^2 + M^2}, \qquad E_{2,+}^l = \sqrt{p_x^2 + p_y^2 + p_z^2 + M^2} \end{aligned} \tag{3.12}$$

where the superscript denotes the degeneracy of the corresponding eigenvalues and m_1, M can act as independent mass terms, satisfying our Dirac-like model. A number of matrix configurations could be constructed by simply rearranging terms, yielding the same eigenvalues.

3.2.1 6×6 Spin-s Representation of $SO(3)$

The dimensionality of the spin-s representation is $2s+1$, thus for the 6×6 case

$$2s + 1 = 6 \Longrightarrow s = \frac{5}{2} \tag{3.13}$$

The following procedure outlined in Sect.(2.0.5) can be used to obtain the following spin matrix representations of the S_i generators

$$\langle \sigma' | \hat{S}_x | \sigma \rangle = \frac{\hbar}{2} \begin{bmatrix} 0 & \sqrt{5} & 0 & 0 & 0 & 0 \\ \sqrt{5} & 0 & 2\sqrt{2} & 0 & 0 & 0 \\ 0 & 2\sqrt{2} & 0 & 3 & 0 & 0 \\ 0 & 0 & 3 & 0 & 2\sqrt{2} & 0 \\ 0 & 0 & 0 & 2\sqrt{2} & 0 & \sqrt{5} \\ 0 & 0 & 0 & 0 & \sqrt{5} & 0 \end{bmatrix} \tag{3.14}$$

$$\langle \sigma' | \hat{S}_y | \sigma \rangle = \frac{i\hbar}{2} \begin{bmatrix} 0 & -\sqrt{5} & 0 & 0 & 0 & 0 \\ \sqrt{5} & 0 & -2\sqrt{2} & 0 & 0 & 0 \\ 0 & 2\sqrt{2} & 0 & -3 & 0 & 0 \\ 0 & 0 & 3 & 0 & -2\sqrt{2} & 0 \\ 0 & 0 & 0 & 2\sqrt{2} & 0 & -\sqrt{5} \\ 0 & 0 & 0 & 0 & \sqrt{5} & 0 \end{bmatrix} \tag{3.15}$$

$$\langle \sigma' | \hat{S}_z | \sigma \rangle = \hbar \begin{bmatrix} 5 & 0 & 0 & 0 & 0 & 0 \\ 0 & 3 & 0 & 0 & 0 & 0 \\ 0 & 0 & 1 & 0 & 0 & 0 \\ 0 & 0 & 0 & -1 & 0 & 0 \\ 0 & 0 & 0 & 0 & -3 & 0 \\ 0 & 0 & 0 & 0 & 0 & -5 \end{bmatrix} \tag{3.16}$$

For 6×6 case, we have explicitly obtained the spin-5/2 representation for $SO(3)$.

3.2.2 6×6 Real Spectra of Energy Dispersion Relations $E(k)$

Using the eigenvalues in (3.12), we plotted the energy dispersion relations $E(k)$ for the 6×6 case using Wolfram Mathematica. It is clear that the plot of the 6×6 real spectra is identical to the 5×5 case. The only difference in the eigenvalues is that the degeneracy of the zero eigenvalue increases by one in the 6×6 case, which makes no visual difference in the actual spectra.

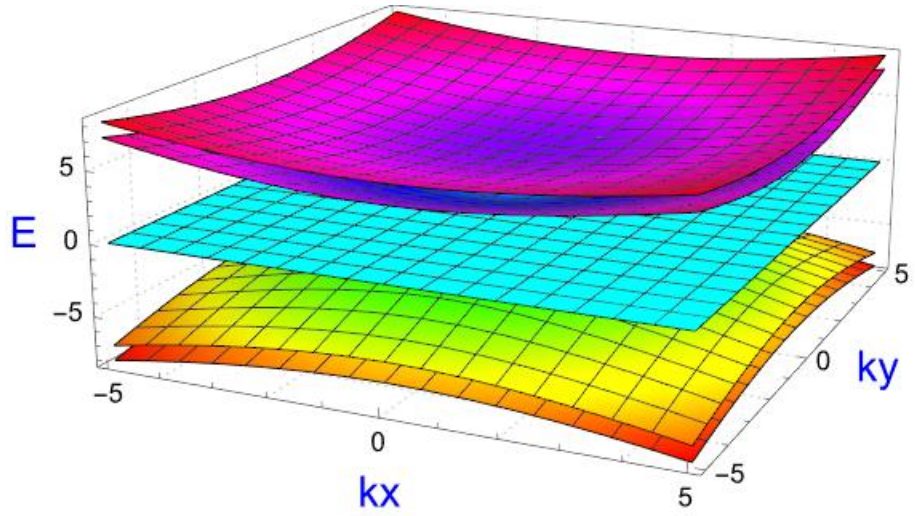

Figure 3.5: The 6×6 real spectra of energy dispersion relations $E(k)$ where $m_1 \neq M$.

The side view of the real spectra is also plotted in order to explicitly see the separation between the energy dispersion relations $E(k)$.

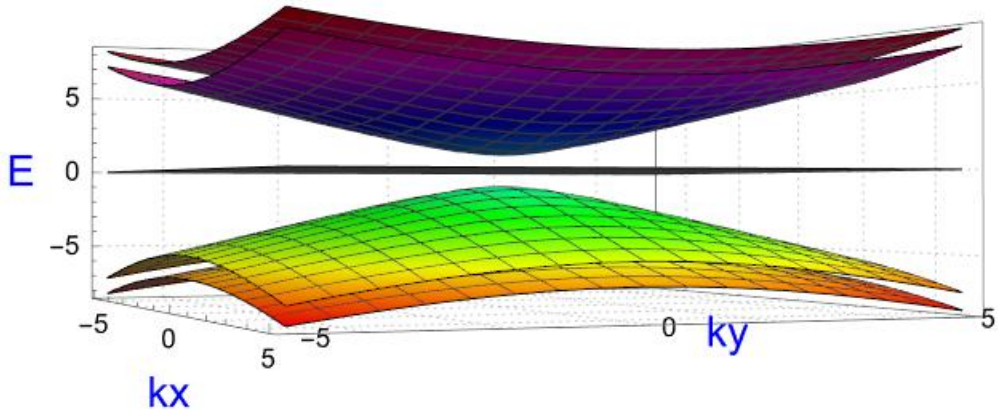

Figure 3.6: Side view of the 6×6 real spectra of energy dispersion relations $E(k)$ where $m_1 \neq M$.

Like the 5×5 case, this resembles the energy dispersion $E(k)$ of A near a threefold degeneracy of exotic fermion types in SGs 199 and 214 in Fig (1.2), as illustrated in [2].

3.3 7×7 Case

Our starting point for the 7×7 case was still motivated by the use of the direct sum. Initially, it involved the Gell-Mann density Hamiltonian as well as the Dirac density

Hamiltonian corresponding to the two independent mass terms, m_1 and m_2 as follows

$$\mathcal{H}_{n=7} = \begin{bmatrix} 0 & p_x + ip_y & 0 & 0 & 0 & 0 & 0 \\ p_x - ip_y & 0 & p_z + im_1 & 0 & 0 & 0 & 0 \\ 0 & p_z - im_1 & 0 & 0 & 0 & 0 & 0 \\ 0 & 0 & 0 & m_2 & 0 & p_z & p_x - ip_y \\ 0 & 0 & 0 & 0 & m_2 & p_x + ip_y & -p_z \\ 0 & 0 & 0 & p_z & p_x - ip_y & -m_2 & 0 \\ 0 & 0 & 0 & p_x + ip_y & -p_z & 0 & -m_2 \end{bmatrix} \tag{3.17}$$

which yielded the following Dirac-like eigenvalues in Eqs. (1.52)

$$\begin{aligned} E_0^1 = 0, \quad E_{1,-}^1 = -\sqrt{p_x^2 + p_y^2 + p_z^2 + {m_1}^2}, \quad E_{1,+}^1 = \sqrt{p_x^2 + p_y^2 + p_z^2 + {m_1}^2} \\ E_{2,-}^2 = -\sqrt{p_x^2 + p_y^2 + p_z^2 + {m_2}^2}, \quad E_{2,+}^2 = \sqrt{p_x^2 + p_y^2 + p_z^2 + {m_2}^2} \end{aligned} \tag{3.18}$$

where the superscript denotes the degeneracy of the corresponding eigenvalues.

Furthermore, we have shown it is possible to build 7×7 matrices without use of the direct sum. Attempting to generalise the examples of matrix (3.1) and matrix (3.9) for the 7×7 case, we have

$$\mathcal{H}_{n=7} = \begin{bmatrix} 0 & p_x + im_1 & 0 & m_2 + im_3 & 0 & 0 & ip_y - p_z \\ p_x - im_1 & 0 & 0 & 0 & 0 & ip_y - p_z & 0 \\ 0 & 0 & 0 & 0 & 0 & 0 & 0 \\ m_2 - im_3 & 0 & 0 & 0 & 0 & m_4 + im_5 & 0 \\ 0 & 0 & 0 & 0 & 0 & 0 & 0 \\ 0 & -ip_y - p_z & 0 & m_4 - im_5 & 0 & 0 & p_x + im_1 \\ -ip_y - p_z & 0 & 0 & 0 & 0 & -p_x - im_1 & 0 \end{bmatrix} \tag{3.19}$$

which yielded the following eigenvalues

$$E = 0, 0, 0, \ \pm\sqrt{p_x^2 + p_y^2 + p_z^2 + {m_1}^2}, \ \pm\sqrt{p_x^2 + p_y^2 + p_z^2 + {m_1}^2 + {m_2}^2 + {m_3}^2 + {m_4}^2 + {m_5}^2} \tag{3.20}$$

in agreement with the desired Dirac-like eigenvalues of Eqs. (1.52).

As outlined in Sect.(2.0.4), the grouping of the mass terms with sufficient free parameters, means we can express

$${m_1}^2 + {m_2}^2 + {m_3}^2 + {m_4}^2 + {m_5}^2 = M^2 \tag{3.21}$$

which yields the resulting eigenvalues

$$\begin{aligned} E_0^3 = 0, \quad E_{1,-}^1 = -\sqrt{p_x^2 + p_y^2 + p_z^2 + {m_1}^2}, \quad E_{1,+}^1 = \sqrt{p_x^2 + p_y^2 + p_z^2 + {m_1}^2} \\ E_{2,-}^1 = -\sqrt{p_x^2 + p_y^2 + p_z^2 + M^2}, \quad E_{2,+}^l = \sqrt{p_x^2 + p_y^2 + p_z^2 + M^2} \end{aligned} \tag{3.22}$$

where the superscript denotes the degeneracy of the corresponding eigenvalues and m_1, M can act as independent mass terms, satisfying our Dirac-like model.

The larger dimensional 7×7 matrix can accommodate the direct sum of two Gell-Mann density Hamiltonians, leading to further configurations which appear more trivial. It simply involves an additional zero row and column, which increases the degeneracy of the zero eigenvalue by one. While it obviously yields the correct eigenvalues, it is otherwise an unsatisfactory approach since it does not feel rewarding given its seemingly trivial nature. At least 27 different matrix configurations can be constructed using this method, which does not seem to introduce any extra information which appears beneficial or useful. This can be generalised to higher dimensional matrices such as the 8×8 case. A number of examples are included in the appendix.

3.3.1 7×7 Spin-s Representation of $SO(3)$

With the dimensionality of the spin-s representation being $2s+1$, the 7×7 case yields

$$2s + 1 = 7 \Longrightarrow s = 3 \tag{3.23}$$

The following procedure outlined in Sect.(2.0.5) can be used to obtain the following spin matrix representations of the S_i generators

$$\langle\sigma'|\,\hat{S}_+\,|\sigma\rangle = \frac{\hbar}{2}\begin{bmatrix} 0 & \sqrt{6} & 0 & 0 & 0 & 0 & 0 \\ \sqrt{6} & 0 & \sqrt{10} & 0 & 0 & 0 & 0 \\ 0 & \sqrt{10} & 0 & 2\sqrt{3} & 0 & 0 & 0 \\ 0 & 0 & 2\sqrt{3} & 0 & 2\sqrt{3} & 0 & 0 \\ 0 & 0 & 0 & \sqrt{10} & 0 & \sqrt{10} & 0 \\ 0 & 0 & 0 & 0 & \sqrt{10} & 0 & \sqrt{6} \\ 0 & 0 & 0 & 0 & 0 & \sqrt{6} & 0 \end{bmatrix} \tag{3.24}$$

$$\langle\sigma'|\,\hat{S}_+\,|\sigma\rangle = \frac{i\hbar}{2}\begin{bmatrix} 0 & -\sqrt{6} & 0 & 0 & 0 & 0 & 0 \\ \sqrt{6} & 0 & -\sqrt{10} & 0 & 0 & 0 & 0 \\ 0 & \sqrt{10} & 0 & -2\sqrt{3} & 0 & 0 & 0 \\ 0 & 0 & 2\sqrt{3} & 0 & -2\sqrt{3} & 0 & 0 \\ 0 & 0 & 0 & \sqrt{10} & 0 & -\sqrt{10} & 0 \\ 0 & 0 & 0 & 0 & \sqrt{10} & 0 & -\sqrt{6} \\ 0 & 0 & 0 & 0 & 0 & \sqrt{6} & 0 \end{bmatrix} \tag{3.25}$$

$$\langle\sigma'|\,\hat{S}_+\,|\sigma\rangle = \hbar\begin{bmatrix} 3 & 0 & 0 & 0 & 0 & 0 & 0 \\ 0 & 2 & 0 & 0 & 0 & 0 & 0 \\ 0 & 0 & 1 & 0 & 0 & 0 & 0 \\ 0 & 0 & 0 & 0 & 0 & 0 & 0 \\ 0 & 0 & 0 & 0 & -1 & 0 & 0 \\ 0 & 0 & 0 & 0 & 0 & -2 & 0 \\ 0 & 0 & 0 & 0 & 0 & 0 & -3 \end{bmatrix} \tag{3.26}$$

For 7×7 case, we have explicitly obtained the spin-3 representation for $SO(3)$.

3.3.2 7×7 Real Spectra of Energy Dispersion Relations $E(k)$

Using the eigenvalues in Eqs. (3.22), we plotted the energy dispersion relations $E(k)$ for the 7×7 case using Wolfram Mathematica. It is clear that the plot of the 7×7 real spectra is identical to the 5×5 case. The only difference in the eigenvalues is that the degeneracy of the zero eigenvalue increases by two in the 7×7 case, which makes no visual difference in the actual spectra.

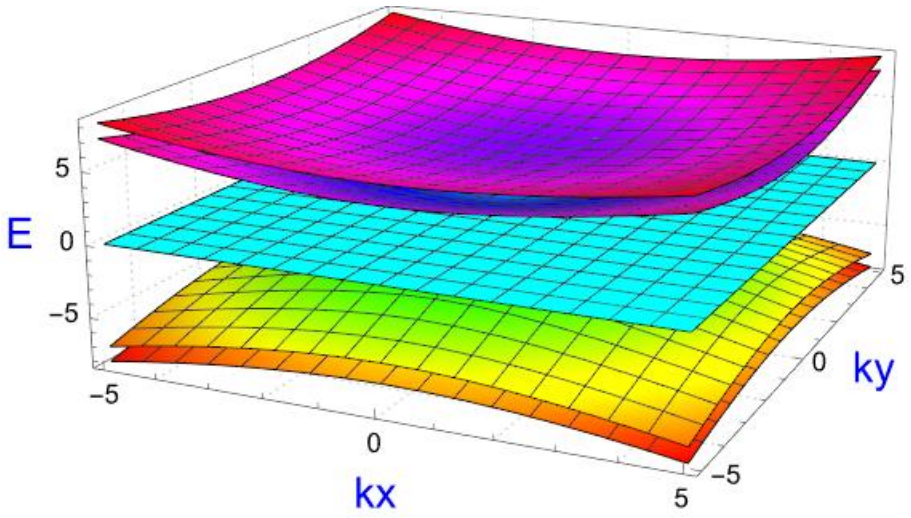

Figure 3.7: The 7×7 real spectra of energy dispersion relations $E(k)$, where $m_1 \neq M$.

The side view of the real spectra is also plotted in order to explicitly see the separation between the energy dispersion relations $E(k)$.

Like the 5×5 and 6×6 cases, this resembles the energy dispersion $E(k)$ of A near a threefold degeneracy of exotic fermion types in SGs 199 and 214 in Fig (1.2), as illustrated in [2].

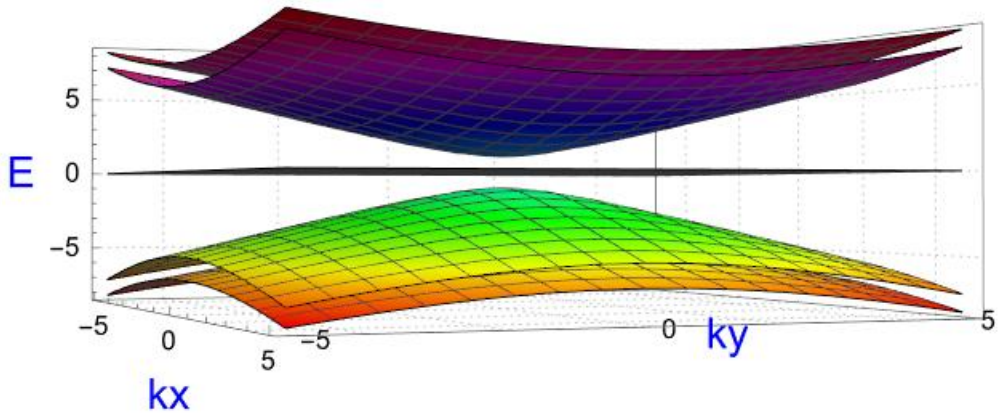

Figure 3.8: Side view of the 7×7 real spectra of energy dispersion relations $E(k)$, where $m_1 \neq M$.

3.4 8×8 Case

The following matrix was included for the sake of completeness, in order to illustrate our chain of reasoning. Systematically, our initial method for the 8×8 case, from the previous cases, involved a direct sum consisting of two Dirac density Hamiltonians, for the two independent masses m_1 and m_2

$$\mathcal{H}_{n=8} = \begin{bmatrix} m_1 & 0 & p_z & p_x - ip_y & 0 & 0 & 0 & 0 \\ 0 & m_1 & p_x + ip_y & -p_z & 0 & 0 & 0 & 0 \\ p_z & p_x - ik_y & -m_1 & 0 & 0 & 0 & 0 & 0 \\ p_x + ip_y & -p_z & 0 & -m_1 & 0 & 0 & 0 & 0 \\ 0 & 0 & 0 & 0 & m_2 & 0 & p_z & p_x - ip_y \\ 0 & 0 & 0 & 0 & 0 & m_2 & p_x + ip_y & -p_Z \\ 0 & 0 & 0 & 0 & p_z & p_x - ip_y & -m_2 & 0 \\ 0 & 0 & 0 & 0 & p_x + ip_y & -p_z & 0 & -m_2 \end{bmatrix} \tag{3.27}$$

which yielded the following eigenvalues

$$\begin{aligned} E = \pm \sqrt{p_x^2 + p_y^2 + p_z^2 + {m_1}^2}, \ \pm \sqrt{p_x^2 + p_y^2 + p_z^2 + {m_1}^2}, \\ \pm \sqrt{p_x^2 + p_y^2 + p_z^2 + {m_2}^2}, \ \pm \sqrt{p_x^2 + p_y^2 + p_z^2 + {m_2}^2} \end{aligned} \tag{3.28}$$

However, since this matrix does not yield the zero eigenvalue, $E = 0$, in accordance to Eqs. (1.52), this $\mathcal{H}_{n=8}$ cannot describe fermions of our Dirac-like model. This is expected since it consists of Dirac density Hamiltonians, which satisfy the Clifford algebra $\mathrm{Cl}_{3,1} \Longrightarrow \{\beta_\mu, \beta_\nu\} = 2\delta_{\mu\nu}\mathbb{1}$. Therefore, this matrix must be abandoned.

Based on previous cases, we anticipated that it is possible to build 8×8 matrices that do not rely on the direct sum. The most notable example is perhaps the generalisation

or extension of the examples shown in matrix (3.1), matrix (3.9) and matrix (3.19) to the 8×8 case. The following example of $\mathcal{H}_{n=8}$ is shown

$$\begin{bmatrix} 0 & p_x + im_1 & 0 & m_2 + im_3 & 0 & 0 & 0 & ip_y - p_z \\ p_x + im_1 & 0 & 0 & 0 & 0 & 0 & ip_y - p_z & 0 \\ 0 & 0 & 0 & m4 + im_5 & p_x + im_1 & ip_y - p_z & 0 & 0 \\ m_2 - im_3 & 0 & m4 - im_5 & 0 & 0 & 0 & m_6 + im_7 & 0 \\ 0 & 0 & p_x - im_1 & 0 & 0 & 0 & 0 & 0 \\ 0 & 0 & -ip_y - p_z & 0 & 0 & 0 & 0 & 0 \\ 0 & -ip_y - p_z & 0 & m_6 - im_7 & 0 & 0 & 0 & -p_x + im_1 \\ -ip_y - p_z & 0 & 0 & 0 & 0 & 0 & -p_x - im_1 & 0 \end{bmatrix} \tag{3.29}$$

which yielded the following eigenvalues

$$\begin{aligned} E = 0,\, 0,\, \pm\sqrt{p_x^2 + p_y^2 + p_z^2 + {m_1}^2},\, \pm\sqrt{p_x^2 + p_y^2 + p_z^2 + {m_1}^2} \\ \pm\sqrt{p_x^2 + p_y^2 + p_z^2 + {m_1}^2 + {m_2}^2 + {m_3}^2 + {m_4}^2 + {m_5}^2 + {m_6}^2 + {m_7}^2} \end{aligned} \tag{3.30}$$

As outlined in Sect.(2.0.4), the grouping of the mass terms with sufficient free parameters, means we can express

$${m_1}^2 + {m_2}^2 + {m_3}^2 + {m_4}^2 + {m_5}^2 + {m_6}^2 + {m_7}^2 = M^2 \tag{3.31}$$

which yields the resulting eigenvalues

$$\begin{aligned} E_0^2 = 0, \quad E_{1,-}^2 = -\sqrt{p_x^2 + p_y^2 + p_z^2 + {m_1}^2}, \quad E_{1,+}^2 = \sqrt{p_x^2 + p_y^2 + p_z^2 + {m_1}^2} \\ E_{2,-}^1 = -\sqrt{p_x^2 + p_y^2 + p_z^2 + M^2}, \quad E_{2,+}^1 = \sqrt{p_x^2 + p_y^2 + p_z^2 + M^2} \end{aligned} \tag{3.32}$$

where the superscript denotes the degeneracy of the corresponding eigenvalues and m_1, M can act as independent mass terms, satisfying our Dirac-like model. A number of matrix configurations could be constructed by simply rearranging terms or exchanging the momenta and mass terms, yielding the same eigenvalues.

The larger dimensional 8×8 matrix can also accommodate the direct sum of either two Gell-Mann density Hamiltonians or one Gell-Mann and one Dirac density Hamiltonian. Despite them clearly producing the required Dirac-like eigenvalues, this leads to more trivial matrices which, as mentioned in the 7×7 case, is rather unsatisfactory. The additional zero rows and columns will simply increase the degeneracy of the zero eigenvalue, with no additional information that will prove useful or interesting.

3.4.1 8×8 Spin-s Representation of $SO(3)$

With the dimensionality of the spin-s representation being $2s+1$, the 8×8 case yields

$$2s + 1 = 8 \Longrightarrow s = \frac{7}{2} \tag{3.33}$$

The following procedure outlined in Sect.(2.0.5) can be used to obtain the following spin matrix representations of the S_i generators

$$\langle\sigma'|\,\hat{S}_x\,|\sigma\rangle = \frac{\hbar}{2}\begin{bmatrix} 0 & \sqrt{7} & 0 & 0 & 0 & 0 & 0 & 0 \\ \sqrt{7} & 0 & 2\sqrt{3} & 0 & 0 & 0 & 0 & 0 \\ 0 & 2\sqrt{3} & 0 & \sqrt{15} & 0 & 0 & 0 & 0 \\ 0 & 0 & \sqrt{15} & 0 & 4 & 0 & 0 & 0 \\ 0 & 0 & 0 & 4 & 0 & \sqrt{15} & 0 & 0 \\ 0 & 0 & 0 & 0 & \sqrt{15} & 0 & 2\sqrt{3} & 0 \\ 0 & 0 & 0 & 0 & 0 & 2\sqrt{3} & 0 & \sqrt{7} \\ 0 & 0 & 0 & 0 & 0 & 0 & \sqrt{7} & 0 \end{bmatrix} \tag{3.34}$$

$$\langle\sigma'|\,\hat{S}_y\,|\sigma\rangle = \frac{i\hbar}{2}\begin{bmatrix} 0 & -\sqrt{7} & 0 & 0 & 0 & 0 & 0 & 0 \\ \sqrt{7} & 0 & -2\sqrt{3} & 0 & 0 & 0 & 0 & 0 \\ 0 & 2\sqrt{3} & 0 & -\sqrt{15} & 0 & 0 & 0 & 0 \\ 0 & 0 & \sqrt{15} & 0 & -4 & 0 & 0 & 0 \\ 0 & 0 & 0 & 4 & 0 & -\sqrt{15} & 0 & 0 \\ 0 & 0 & 0 & 0 & \sqrt{15} & 0 & -2\sqrt{3} & 0 \\ 0 & 0 & 0 & 0 & 0 & 2\sqrt{3} & 0 & -\sqrt{7} \\ 0 & 0 & 0 & 0 & 0 & 0 & \sqrt{7} & 0 \end{bmatrix} \tag{3.35}$$

$$\langle\sigma'|\,\hat{S}_z\,|\sigma\rangle = \hbar\begin{bmatrix} 7 & 0 & 0 & 0 & 0 & 0 & 0 & 0 \\ 0 & 5 & 0 & 0 & 0 & 0 & 0 & 0 \\ 0 & 0 & 3 & 0 & 0 & 0 & 0 & 0 \\ 0 & 0 & 0 & 1 & 0 & 0 & 0 & 0 \\ 0 & 0 & 0 & 0 & -1 & 0 & 0 & 0 \\ 0 & 0 & 0 & 0 & 0 & -3 & 0 & 0 \\ 0 & 0 & 0 & 0 & 0 & 0 & -5 & 0 \\ 0 & 0 & 0 & 0 & 0 & 0 & 0 & -7 \end{bmatrix} \tag{3.36}$$

For 8×8 case, we have explicitly obtained the spin-7/2 representation for $SO(3)$.

3.4.2 8×8 Real Spectra of Energy Dispersion Relations $E(k)$

Using the eigenvalues in (3.32), we plotted the energy dispersion relations $E(k)$ for the 8×8 case using Wolfram Mathematica. This differs from the previous cases by having two additional eigenvalues associated with m_1. However, it makes no visual difference, as the extra dispersion relations overlap exactly with each other. As usual, there is greater separation between the energy dispersions, as you increase the difference between the independent mass terms.

The side view of the real spectra is also plotted in order to explicitly see the separation between the energy dispersion relations $E(k)$.

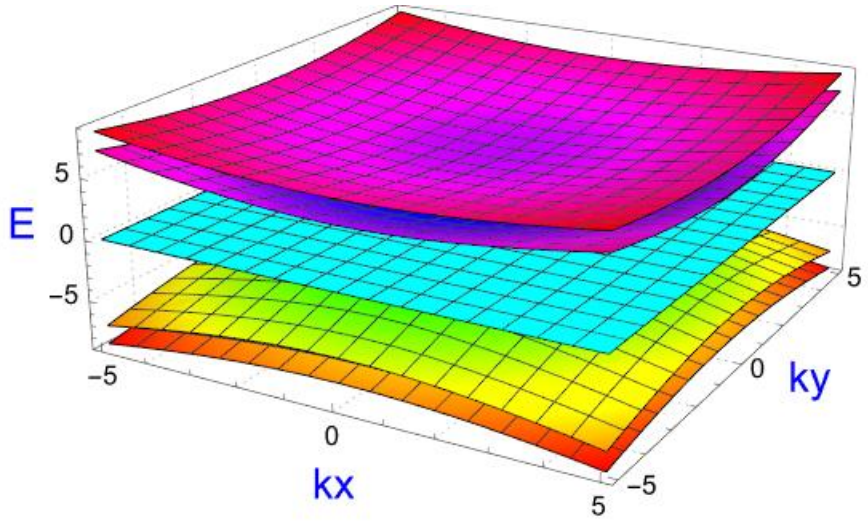

Figure 3.9: The 8×8 real spectra of the energy dispersion relations $E(k)$, where $m_1 \neq M$.

Likewise, this resembles the energy dispersion $E(k)$ of A near a threefold degeneracy of exotic fermion types in SGs 199 and 214 in Fig (1.2), as illustrated in [2].

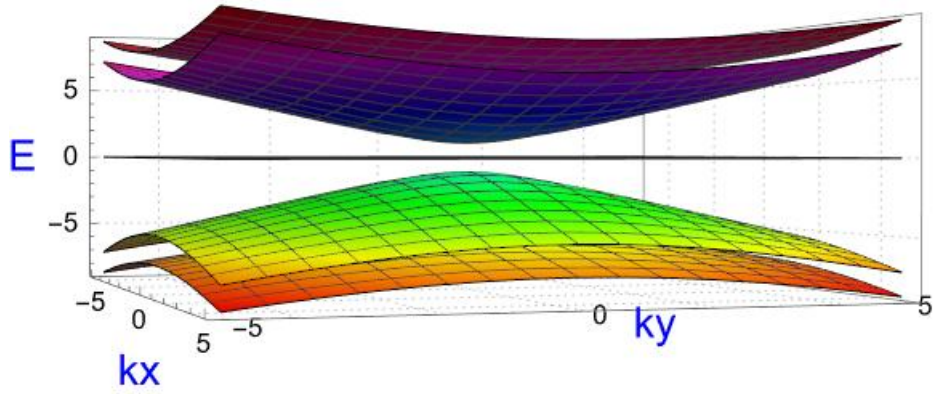

Figure 3.10: Side view of the 8×8 real spectra of the energy dispersion relations $E(k)$.

3.4.3 Possible Third Mass Term m_3

The 8×8 case is perhaps the most interesting case to study for $5 \leq n \leq 8$. So far, this is the only case where we were able to build a matrix that incorporated a third independent mass term, m_3. The resulting expression for the density Hamiltonian $\mathcal{H}_{n=8}$ is outlined in matrix (3.37). The construction of such a matrix is heavily influenced by matrix (3.29), which involves a substitution of m_2 and minimal rearrangement of

the matrix elements, as follows

$$\begin{bmatrix} 0 & p_x+im_1 & 0 & m_2+im_3 & 0 & 0 & 0 & ip_y-p_z \\ p_x-im_1 & 0 & 0 & 0 & 0 & 0 & ip_y-p_z & 0 \\ 0 & 0 & 0 & 0 & p_x+im_2 & ip_y-p_z & 0 & 0 \\ m_2-im_3 & 0 & 0 & 0 & 0 & 0 & m_4+im_5 & 0 \\ 0 & 0 & p_x-im_2 & 0 & 0 & 0 & 0 & 0 \\ 0 & 0 & -ip_y-p_z & 0 & 0 & 0 & 0 & 0 \\ 0 & -ip_y-p_z & 0 & m_4-im_5 & 0 & 0 & 0 & -p_x+im_1 \\ -ip_y-p_z & 0 & 0 & 0 & 0 & 0 & -p_x-im_1 & 0 \end{bmatrix} \tag{3.37}$$

which yielded the following eigenvalues

$$\begin{aligned} E = 0,\, 0,\, \pm\sqrt{p_x^2+p_y^2+p_z^2+{m_1}^2},\, \pm\sqrt{p_x^2+p_y^2+p_z^2+{m_2}^2} \\ \pm\sqrt{p_x^2+p_y^2+p_z^2+{m_1}^2+{m_2}^2+{m_3}^2+{m_4}^2+{m_5}^2} \end{aligned} \tag{3.38}$$

As outlined in Sect.(2.0.4), the grouping of the mass terms with sufficient free parameters, means we can express the following

$${m_1}^2+{m_2}^2+{m_3}^2+{m_4}^2+{m_5}^2 = M^2$$

which yields the resulting eigenvalues

$$\begin{aligned} E_0^2 = 0, \quad E_{1,-}^1 &= -\sqrt{p_x^2+p_y^2+p_z^2+{m_1}^2}, \quad E_{1,+}^1 = \sqrt{p_x^2+p_y^2+p_z^2+{m_1}^2} \\ E_{2,-}^1 &= -\sqrt{p_x^2+p_y^2+p_z^2+{m_2}^2}, \quad E_{2,+}^1 = \sqrt{p_x^2+p_y^2+p_z^2+{m_2}^2} \\ E_{3,-}^1 &= -\sqrt{p_x^2+p_y^2+p_z^2+M^2}, \quad E_{3,+}^1 = \sqrt{p_x^2+p_y^2+p_z^2+M^2} \end{aligned} \tag{3.39}$$

where the superscript denotes the degeneracy of the corresponding eigenvalues and m_1, m_2, M can act as three independent mass terms, satisfying our Dirac-like model. By rearranging elements, we obtained four 8×8 matrices that incorporated β_6, yielding a third mass term m_3.

3.4.4 8×8 Real Spectra involving m_3

Using the eigenvalues in Eqs. (3.39), we plotted the energy dispersion relations $E(k)$ for the 8×8 case using Wolfram Mathematica. This is clearly the most distinct plot with the inclusion of the third mass term. Compared to the previous plots, there are seven energy dispersions which are clearly visible with the zero eigenvalue doubly degenerate. As usual, there is greater separation between the energy dispersions, as you increase the difference between the independent mass terms.

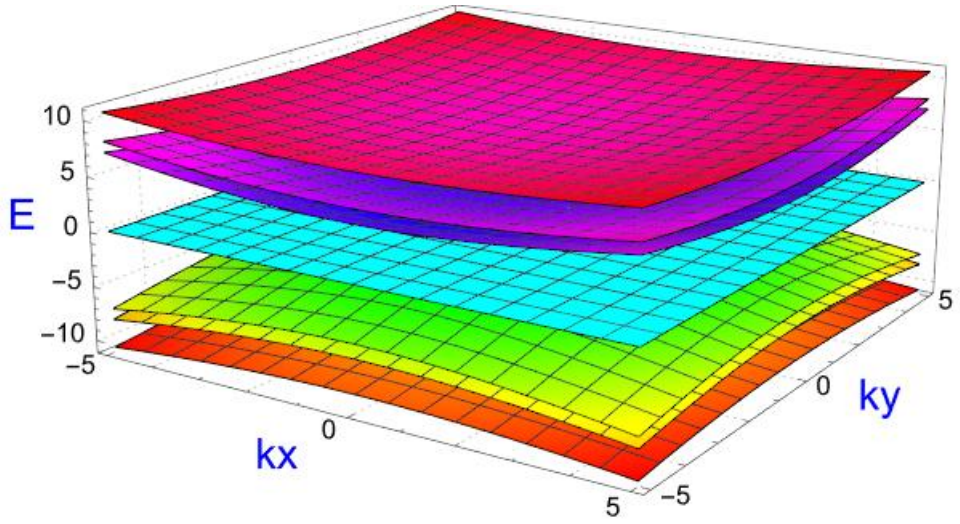

Figure 3.11: The 8×8 real spectra of the energy dispersion relations $E(k)$ where $m_1 \neq m_2 \neq M$.

The side view of the real spectra is also plotted in order to explicitly see the separation between the energy dispersion relations $E(k)$

Likewise, this resembles the energy dispersion $E(k)$ of A near a threefold degeneracy of exotic fermion types in SGs 199 and 214 in Fig (1.2), as illustrated in [2].

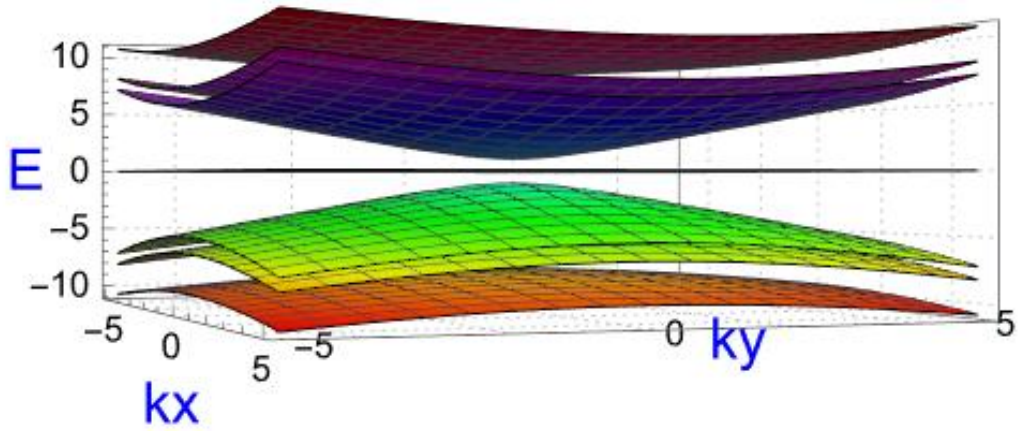

Figure 3.12: Side view of the 8×8 real spectra of the energy dispersion relations $E(k)$ where $m_1 \neq m_2 \neq M$.

Chapter 4

Conclusion

Our proposed Dirac-like model in 3+1 dimensions was constructed in order to describe exotic and unconventional fermionic particles. The natural arena for the discovery of such particles is within condensed matter systems, which impose symmetry laws that are less constrained than relativistic particles, diversifying the type of particles that can occur. This leads to the potential to classify fermions that lie outside the standard categories of Dirac, Majorana and Weyl fermions, according to QFT. The density Hamiltonian $\mathcal{H}$ of our Dirac-like model is composed of $n \times n$ matrices β_μ associated with the momenta, $p_i = p_x, p_y, p_z$, and the independent mass terms m_1 and m_2. These yield the energies of our fermionic system upon diagonalisation of $\mathcal{H}$, expressed as the standard relativistic energy-momentum relations in Eqs. (1.52). In essence, the main goal of the project was to construct these $n \times n$ matrices for $5 \leq n \leq 8$. For each n, we also constructed the explicit spin matrices of S_i generators for the spin-s representation of the SO(3) gauge group. We managed to achieve more than fifty matrix configurations for the $n \times n$ cases, albeit there were more trivial cases for the higher dimensional matrices, most notably the 7×7 and 8×8 cases. Despite obtaining a substantial number of matrices, progress still needs to be made in order to construct a general method of building such Dirac-like matrices. The most noteworthy $\mathcal{H}$ configurations for the 5×5 and 6×6 cases (matrices (3.1) and (3.9) respectively), delightfully proposed by our brilliant supervisor Gian, had undergone attempted generalisation to the 7×7 and 8×8 cases (matrices (3.19) and (3.29) respectively), which we feel was somewhat successful. The real spectra of the energy dispersion relations $E(k)$, were plotted using Wolfram Mathematica for each $n \times n$ case, which appeared to resemble the $E(k)$ of A as seen in Fig. (1.2). Furthermore, one of the goals was to construct a possible β_6 matrix associated with a third independent mass term, m_3, which we accomplished for the 8×8 case as seen in matrix (3.37). The possibility of obtaining β_6 for cases $n = 5, 6, 7$ has not been ruled out, which therefore merits further study. The general method of building such matrices would be predicated upon discovering the algebra, especially the anti-commutation relations that β_μ would satisy, which is also an area of further study.

One of the most startling results obtained was the non-Hermitian density Hamiltonian $\mathcal{H}_{n=5}$ in the 5×5 case as outlined in Sect.(3.1.1). This prompted an unprecedented venture into the realm of non-Hermitian quantum mechanics or pseudo-Hermitian QM, in which a specific system would be parity-time ($\mathcal{PT}$) symmetry. If we consider a wavefunction $\psi(x)$, then parity, the spatial inversion operator $\mathcal{P}$, and the time reversal operator, $\mathcal{T}$, can be applied as

$$\mathcal{P}\psi(x) = \psi(-x) \qquad\qquad \mathcal{T}\psi(x) = \psi(x)^* \tag{4.1}$$

The $\mathcal{PT}$ symmetry imposes a constraint which will lead to a real spectrum despite the non-Hermiticity property, a complete set of $\mathcal{PT}$ invariant eigenvectors. Mostafazadeh showed that a non-Hermitian Hamiltonian endowed with a real spectrum is pseudo-Hermitian [4].

One possible direction to research is to consider the situation of restricting the momentum components of the fermion to 2+1 dimensions or 1+1 dimensions. If we consider for instance, the 1+1 dimensional system which serves as a ground for the discovery of Majorana fermions, it can constitute a more varied non-Abelian statistical nature. This can also serve as potential use for topological quantum computing, just as in the case of substitution of the Majorana basis into the Kitaev Hamiltonian of the 1-D fermionic chain [6].

Potentially, what was reviewed and investigated here poses substantial interest and activity for modern day research, with the most notable physical environment being solid state systems. However as previously mentioned, there is still progress to undertake, regarding our proposed Dirac-like model in 3+1 dimensions which would include algebra, general theory, precise applications to band models, etc. Although, we experienced an introductory immersion into emergent quasiparticles and exotic fermion types, the nature and potential applications of such particles is compelling enough to warrant further research and specialisation into the wonderful realm of condensed matter physics.

References

[1] V. Mourik et al., Signatures of Majorana Fermions in Hybrid Superconductor-Semiconductor Nanowire Devices. Science 336, 1003-1007 (2012). doi: 10.1126/science.1222360.

[2] B. Bradlyn et al., Beyond Dirac and Weyl fermions: Unconventional quasiparticles in conventional crystals. Science 353, aaf5037 (2016). doi: 10.1126/science.aaf5037.

[3] S. Esposito, Searching for an equation: Dirac, Majorana and the others, pp. 1-4, `https://arxiv.org/abs/1110.6878v1`, (2011).

[4] A. Mostafazadeh, Pseudo-Hermiticity versus PT Symmetry: The necessary condition for the reality of the spectrum of a non-Hermitian Hamiltonian, `https://arxiv.org/abs/math-ph/0107001` (2002).

[5] D. Tong, Quantum Field Theory: University of Cambridge Part III Mathematical Tripos, pp. 81-90, `http://www.damtp.cam.ac.uk/user/tong/qft/qft.pdf`, (2006).

[6] Dr. Mitchell's physics channel. "Topological quantum matter". *YouTube* video, 2:22:46. April 28, 2020. `https://www.youtube.com/watch?v=ynVqhvSV6x4&list\=PLotxEOxVaaoKRXdDN-7lI3Y88PaHqyOZL&index=18`

[7] J. Maldacena and D. Stanford, Comments on the Sachdev-Ye-Kitaev model, `https://arxiv.org/abs/1604.07818` (2016).

[8] R. A. Krajcik and M. M. Nieto, Bhabha first-order wave equations: I. C, P, and T, Phys. Rev. D 10, 4049, (1974). doi: 10.1103/PhysRevD.10.4049

[9] R. A. Krajcik and M. M. Nieto, Bhabha first-order wave equations. II. Mass and spin composition, Hamiltonians, and general Sakata-Taketani reductions, Phys. Rev. D 11, 1442, (1974). doi: 10.1103/PhysRevD.11.1442

[10] R. A. Krajcik and M. M. Nieto, Bhabha first-order wave equations. III. Poincare generators, Phys. Rev. D 11, 1459, (1975). doi: 10.1103/PhysRevD.11.1459

Appendix A

A.1 Other Matrix Examples Obtained

A.1.1 6×6

$$\mathcal{H}_{n=6} = \begin{bmatrix} 0 & p_x + ip_y & 0 & 0 & 0 & 0 \\ p_x - ip_y & 0 & 0 & p_z + im_1 & 0 & 0 \\ 0 & 0 & 0 & 0 & p_z + im_2 & 0 \\ 0 & p_z - im_1 & 0 & 0 & i & 0 \\ 0 & 0 & p_z - im_2 & 0 & 0 & p_x + ip_y \\ 0 & 0 & 0 & 0 & p_x - ip_y & 0 \end{bmatrix} \tag{A.1}$$

$$\mathcal{H}_{n=6} = \begin{bmatrix} 0 & 0 & p_z + im_1 & 0 & p_x + ip_y & 0 \\ 0 & 0 & 0 & p_x + ip_y & 0 & 0 \\ p_z - im_1 & 0 & 0 & 0 & 0 & 0 \\ 0 & p_x - ip_y & 0 & 0 & 0 & p_z + im_2 \\ p_x - ip_y & 0 & 0 & 0 & 0 & 0 \\ 0 & 0 & 0 & p_z - im_2 & 0 & 0 \end{bmatrix} \tag{A.2}$$

$$\mathcal{H}_{n=6} = \begin{bmatrix} 0 & p_x + im_1 & p_y + ip_z & 0 & 0 & 0 \\ p_x - im_1 & 0 & 0 & 0 & 0 & 0 \\ p_y - ip_z & 0 & 0 & 0 & 0 & 0 \\ 0 & 0 & 0 & 0 & 0 & p_y + ip_z \\ 0 & 0 & 0 & 0 & 0 & p_x + im_2 \\ 0 & 0 & 0 & p_y - ip_z & p_x - im_2 & 0 \end{bmatrix} \tag{A.3}$$

$$\mathcal{H}_{n=6} = \begin{bmatrix} 0 & p_x + im_1 & 0 & p_y + ip_z & 0 & 0 \\ p_x - im_1 & 0 & 0 & 0 & 0 & 0 \\ 0 & 0 & 0 & 0 & 0 & p_y + ip_z \\ p_y - ip_z & 0 & 0 & 0 & 0 & 0 \\ 0 & 0 & 0 & 0 & 0 & p_x + im_2 \\ 0 & 0 & p_y - ip_z & 0 & p_x - im_2 & 0 \end{bmatrix} \tag{A.4}$$

A.1.2 7×7

Examples which include the more 7×7 trivial cases as mentioned in Sect.(3.3), initiated from the direct sum of two density Hamiltonians constructed from the Gell-Mann matrices $\lambda_{i=1,2,6,7}$, yielding one additional zero row and column. At least 27 matrices could be obtained by moving different element positions and exchanging momenta and mass terms.

$$\mathcal{H}_{n=7} = \begin{bmatrix} 0 & p_x + ip_y & 0 & 0 & 0 & 0 & 0 \\ p_x - ip_y & 0 & p_z + im_1 & 0 & 0 & 0 & 0 \\ 0 & p_z - im_1 & 0 & 0 & 0 & 0 & 0 \\ 0 & 0 & 0 & 0 & 0 & 0 & 0 \\ 0 & 0 & 0 & 0 & 0 & p_x + ip_y & 0 \\ 0 & 0 & 0 & 0 & p_x - ip_y & 0 & p_z + im_2 \\ 0 & 0 & 0 & 0 & 0 & p_z - im_2 & 0 \end{bmatrix} \tag{A.5}$$

$$\mathcal{H}_{n=7} = \begin{bmatrix} 0 & 0 & p_z + im_1 & 0 & 0 & 0 & 0 \\ 0 & 0 & 0 & 0 & 0 & p_x + ip_y & 0 \\ p_z - im_1 & 0 & 0 & 0 & p_x + ip_y & 0 & 0 \\ 0 & 0 & 0 & 0 & 0 & 0 & 0 \\ 0 & 0 & p_x - ip_y & 0 & 0 & 0 & 0 \\ 0 & p_x - ip_y & 0 & 0 & 0 & 0 & p_z + im_2 \\ 0 & 0 & 0 & 0 & 0 & p_z - im_2 & 0 \end{bmatrix} \tag{A.6}$$

$$\mathcal{H}_{n=7} = \begin{bmatrix} 0 & p_x + im_1 & 0 & 0 & p_y + ip_z & 0 & 0 \\ p_x - im_1 & 0 & 0 & 0 & 0 & 0 & 0 \\ 0 & 0 & 0 & 0 & 0 & 0 & 0 \\ 0 & 0 & 0 & 0 & 0 & p_z + im_2 & 0 \\ p_y - ip_z & 0 & 0 & 0 & 0 & 0 & 0 \\ 0 & 0 & 0 & p_z - im_2 & 0 & 0 & p_y + ip_z \\ 0 & 0 & 0 & 0 & 0 & p_y - ip_z & 0 \end{bmatrix} \tag{A.7}$$

$$\mathcal{H}_{n=7} = \begin{bmatrix} 0 & 0 & p_z + im_1 & 0 & 0 & 0 & p_x + ip_y \\ 0 & 0 & 0 & 0 & 0 & p_x + ip_y & 0 \\ p_z - im_1 & 0 & 0 & 0 & 0 & 0 & 0 \\ 0 & 0 & 0 & 0 & 0 & 0 & 0 \\ 0 & 0 & 0 & 0 & 0 & p_z + im_2 & 0 \\ 0 & p_x - ip_y & 0 & 0 & p_z - im_2 & 0 & 0 \\ p_x - ip_y & 0 & 0 & 0 & 0 & 0 & 0 \end{bmatrix} \tag{A.8}$$

A.1.3 8×8

Examples include the more trivial 8×8 cases, initiated from the direct sum of one Gell-Mann density Hamiltonian and one Dirac density Hamiltonian (one additional zero row and column), followed by the direct sum of two Gell-Mann density Hamiltonians (two additional zero row and columns) in Sect.(3.4). A substantial number of the matrices could be obtained by moving different element positions and exchanging momenta and mass terms.

$$\mathcal{H}_{n=8} = \begin{bmatrix} 0 & p_x + ip_y & 0 & 0 & 0 & 0 & 0 & 0 \\ p_x - ip_y & 0 & p_z + im_1 & 0 & 0 & 0 & 0 & 0 \\ 0 & p_z - im_1 & 0 & 0 & 0 & 0 & 0 & 0 \\ 0 & 0 & 0 & 0 & 0 & 0 & 0 & 0 \\ 0 & 0 & 0 & 0 & m_2 & 0 & p_z & p_x - ip_y \\ 0 & 0 & 0 & 0 & 0 & m_2 & p_x + ip_y & -p_Z \\ 0 & 0 & 0 & 0 & p_z & p_x - ip_y & -m_2 & 0 \\ 0 & 0 & 0 & 0 & px + ip_y & -p_z & 0 & -m_2 \end{bmatrix} \tag{A.9}$$

$$\mathcal{H}_{n=8} = \begin{bmatrix} 0 & p_x - ip_y & 0 & p_z + im_1 & 0 & 0 & 0 & 0 \\ p_x - ip_y & 0 & 0 & 0 & 0 & 0 & 0 & 0 \\ 0 & 0 & 0 & 0 & 0 & 0 & 0 & 0 \\ p_z - im_1 & 0 & 0 & 0 & 0 & 0 & 0 & 0 \\ 0 & 0 & 0 & 0 & m_2 & 0 & p_z & p_x - ip_y \\ 0 & 0 & 0 & 0 & 0 & m_2 & p_x + ip_y & -p_Z \\ 0 & 0 & 0 & 0 & p_z & p_x - ip_y & -m_2 & 0 \\ 0 & 0 & 0 & 0 & px + ip_y & -p_z & 0 & -m_2 \end{bmatrix} \tag{A.10}$$

$$\mathcal{H}_{n=8} = \begin{bmatrix} 0 & p_x + im_2 & 0 & 0 & 0 & 0 & 0 & p_y + ip_z \\ p_x - im_2 & 0 & 0 & 0 & 0 & 0 & p_y + ip_z & 0 \\ 0 & 0 & 0 & 0 & 0 & p_y + ip_z & 0 & 0 \\ 0 & 0 & 0 & 0 & 0 & p_x + im_1 & 0 & 0 \\ 0 & 0 & 0 & 0 & 0 & 0 & 0 & 0 \\ 0 & 0 & p_y - ip_z & p_x - im_1 & 0 & 0 & 0 & 0 \\ 0 & p_y - ip_z & 0 & 0 & 0 & 0 & 0 & -p_x + im_2 \\ p_y - ip_z & 0 & 0 & 0 & 0 & 0 & -p_x - im_2 & 0 \end{bmatrix} \tag{A.11}$$

$$\mathcal{H}_{n=8} = \begin{bmatrix} 0 & p_x + im_2 & 0 & 0 & 0 & 0 & 0 & p_y + ip_z \\ p_x - im_2 & 0 & 0 & 0 & 0 & 0 & p_y + ip_z & 0 \\ 0 & 0 & 0 & p_x + im_1 & 0 & p_y + ip_z & 0 & 0 \\ 0 & 0 & p_x - im_1 & 0 & 0 & 0 & 0 & 0 \\ 0 & 0 & 0 & 0 & 0 & 0 & 0 & 0 \\ 0 & 0 & p_y - ip_z & 0 & 0 & 0 & 0 & 0 \\ 0 & p_y - ip_z & 0 & 0 & 0 & 0 & 0 & -p_x + im_2 \\ p_y - ip_z & 0 & 0 & 0 & 0 & 0 & -p_x - im_2 & 0 \end{bmatrix} \tag{A.12}$$

$$\mathcal{H}_{n=8} = \begin{bmatrix} 0 & p_x + ip_y & 0 & 0 & 0 & 0 & 0 & 0 \\ p_x - ip_y & 0 & p_z + im_1 & 0 & 0 & 0 & 0 & 0 \\ 0 & p_z - im_1 & 0 & 0 & 0 & 0 & 0 & 0 \\ 0 & 0 & 0 & 0 & 0 & 0 & 0 & 0 \\ 0 & 0 & 0 & 0 & 0 & 0 & 0 & 0 \\ 0 & 0 & 0 & 0 & 0 & 0 & p_x + ip_y & 0 \\ 0 & 0 & 0 & 0 & 0 & p_x + ip_y & 0 & p_z + im_2 \\ 0 & 0 & 0 & 0 & 0 & 0 & p_z - im_2 & 0 \end{bmatrix} \tag{A.13}$$

$$\mathcal{H}_{n=8} = \begin{bmatrix} 0 & p_x + im_1 & 0 & 0 & 0 & p_y + ip_z & 0 & 0 \\ p_x - im_1 & 0 & 0 & 0 & 0 & 0 & p_y + ip_z & 0 \\ 0 & 0 & 0 & 0 & 0 & 0 & 0 & 0 \\ 0 & 0 & 0 & 0 & 0 & 0 & 0 & 0 \\ 0 & 0 & 0 & 0 & 0 & 0 & 0 & 0 \\ 0 & p_y - ip_z & 0 & 0 & 0 & 0 & 0 & 0 \\ 0 & 0 & p_y - ip_z & 0 & 0 & 0 & 0 & p_x + im_2 \\ 0 & 0 & 0 & 0 & 0 & 0 & p_x - im_2 & 0 \end{bmatrix} \tag{A.14}$$

$$\mathcal{H}_{n=8} = \begin{bmatrix} 0 & 0 & p_z + im_1 & 0 & 0 & 0 & 0 & p_x + ip_y \\ 0 & 0 & 0 & 0 & 0 & 0 & p_x + ip_y & 0 \\ p_z - im_1 & 0 & 0 & 0 & 0 & 0 & 0 & 0 \\ 0 & 0 & 0 & 0 & 0 & 0 & 0 & 0 \\ 0 & 0 & 0 & 0 & 0 & 0 & 0 & 0 \\ 0 & 0 & 0 & 0 & 0 & 0 & p_z + im_2 & 0 \\ 0 & p_x - ip_y & 0 & 0 & 0 & p_z - im_2 & 0 & 0 \\ p_x - ip_y & 0 & 0 & 0 & 0 & 0 & 0 & 0 \end{bmatrix} \tag{A.15}$$